1-1-2013

Tidal Flux of Trace Metals and Rare Earth Elements in a Barrier Island Salt Marsh

Ryan Antle
University of South Carolina

Tidal Flux of Trace Metals and Rare Earth Elements in a Barrier Island Salt Marsh

By

Ryan Antle

Bachelor of Sciences
University of South Carolina, 2011

Submitted in Partial Fulfillment of the Requirements

For the Degree of Master of Science in

Geological Science

College of Arts and Sciences

University of South Carolina

2103

Accepted by:

Michael Bizimis, Major Professor

Seth John, Reader

Sarah Rothenberg, Reader

Alicia Wilson, Reader

Lacy Ford, Vice Provost and Dean of Graduate Studies

Abstract

Barrier island salt marshes are known as sources of nutrients to the coastal ocean but it is unclear whether they are also sources or sinks of trace metals in regards to coastal waters. Salt marshes are characterized by steep redox and biogeochemical gradients, which constantly fluctuate as a result of tidal pumping. While several studies have examined metal budgets between terrestrial fresh water, estuarine subterranean fluids, and coastal saline waters, there is little data regarding fluid chemistry for metals in salt water estuaries in the absence of fresh water input. This study investigated a back barrier salt marsh on Cabretta Island, Ga. This salt marsh has no terrestrial freshwater input component, eliminating potential sources and long range transport of metals from outside the system. As such, the Cabretta salt marsh allows determination of the dissolved flux of metals into coastal seawater from the salt marsh sediments as a result of tidal pumping. This study determined the dissolved (<0.15μm) element concentrations in subterranean fluids and the tidal creek over two ebbing tides, using a new method that allows the simultaneous determination of rare earth elements and transition metals, by a combined isotope dilution and external calibration in small volume (<30mL) saline fluids. We determined elements that are redox sensitive (Fe, Mn, U, Ce, S), biogeochemically reactive (Ni, Cu, Co, Zn, Hg, Pb, Ba, Sr, Ca, Mg), and particle reactive (REE) in order to constrain their cycling between coastal water and the salt marsh. The data shows mixing between subterranean fluids and coastal water end-member components in the tidal creek.

Using Mn, U and Ni as best proxies for mixing, the data shows a larger fraction of the subterranean fluid component in the creek waters at low tide (35%) vs. high tide (5%), consistent with tidal pumping. Mixing calculations between coastal water and average subterranean fluids suggest a highly non-conservative behavior for Fe, consistent with rapid precipitation during export from the marsh. Similar trends with Fe were seen for particle reactive elements, like REE and Pb, suggesting a coupling between Fe precipitation and removal of highly particle reactive elements. Chalcophile elements such as Cu and Zn do not show a correlation with sulfur contents as has been previously thought for these systems, suggesting limited influence of sulfide precipitation in the dissolved budgets of these elements. Flux calculations suggest that during tidal pumping, salt marsh fluids export Mn, Ni, Fe, REE, Pb and to a lesser extent Cu to the tidal creek waters, while the marsh is a sink for U. There is relatively little change in Zn, Ba Mg, and Ca concentrations between fluids and open coastal water. Therefore, barrier island salt marshes, although transient geomorphological features of the coast, may be an underestimated source of metals to the coastal water dissolved metal budget.

Table of Contents

List of Tables

List of Figures

1. Introduction

Tidal marshes include a wide variety of coastal ecological systems that are characterized by their interaction with terrestrial and coastal waters with dynamic ranges of salinity. Marshes are depositional habitats controlled by tidal pumping which inundates and exposes the system daily (Adam, 1990). Due to the relatively slow migration of tides and the protection of marshes from wave action and high river discharge, these systems provide a low energy environment for sediment deposition (Stumpf, 1983). These sediments stabilize large plant communities which are dominated by cord grasses with varying salinity tolerances (Gillham, 1957). These grasses provide nutrients to the marsh ecological system, which supports microbes, algae, juvenile and resident fish species. Because of their high productivity, these ecosystems have been observed as exporters of nutrients to the coastal ocean (Valiela, 1978; Haines, 1979).

Although salt marshes are known sources for nutrients, the cycling of trace metals in marshes is less clear. The fate of metals in these systems is complex due the various reactive properties of metals and dynamic redox gradients in the organic rich marsh sediments (figure 1.1). The metals of interest include redox sensitive metals (Fe, Mn, U), transition metals (Co, Ni, Cu, Zn, Cd, Pb) which form highly insoluble sulfides that are known to be stable in reduced subterranean fluids (SF) and sediments (Koretsky et al, 2008), alkaline earth metals (Ca, Mg, Ba, Sr) which are conservative in seawater and should follow salinity, and rare earth elements (REE) which are particle reactive and, in

the case of Ce, redox sensitive. This study focuses on the water chemistry at the salt marsh-open water interface and includes analysis of dissolved water concentrations from subterranean fluids (SF), tidal creek, and the coastal waterway. By measuring the tidal creek over an ebbing tide, this study constrains whether the reduced marsh fluids are a source or a sink for the above range of metals to the coastal water. Emphasis was placed on the interface between the subterranean marsh fluids and the tidal creek so as to constrain the metal fluxes between the reduced SF and open water.

An important component of this study also was the development of a method for the determination of all the above elements in saline fluids in a single comprehensive analytical method**.** In order to determine metals that vary both in reactivity and relative abundance, an existing method for the extraction of transition elements was refined with the addition of REEs, Mg, Ca, Sr, Ba, and U.

1.1 Salt Marshes: Sources or Sinks?

Salt marshes are known as net exporters of nutrients to coastal waters, and some studies have investigated metal fluxes in similar environments. For example, uranium has been shown to be sequestered by salt marsh sediments. It was hypothesized that as seawater infiltrates the sediments and becomes reduced, uranium is removed from the pore fluids due to the insolubility of U(IV) (Church et al, 1996).

Other studies have looked at the abundance of Mn, Cu, Ni, Co, Pb, Fe, Ba, & Sr in SF in marsh systems (Duncan & Shaw, 2003; Charette & Sholkovitz, 2005; Beck et al, 2006 Korestsky et al., 2008; Santos-Echeandía et al., 2010). The studies found that these elements are highly variable in the marsh pore fluids. This variability is controlled by depth, location from the creek, and changes in plant zonation. Although Duncan & Shaw

(2003) & Charette & Sholkovitz (2005) examined deep wells (>2m) and Beck et al (2006) measured surface pore fluids (<50cm) all attempted to constrain the fluxes of these elements to the overlying coastal waters by using general groundwater flow models and the determined concentrations. Santos-Echeandía et al. (2010) examined the effect of tidal flooding on the upward migration of metals from the shallow sediments (<25cm) to determine fluxes. In every case, their estimates were based on high subterranean fluid concentrations which leave the system by horizontal groundwater flow or horizontal surface flow. In these studies, marshes were sources of metals (Fe and Mn) to the coastal ocean. However, the redox gradients at the Cabretta barrier island salt marsh may not permit these metals to migrate into the tidal creek unimpeded as these studies assume. In order to more accurately constrain the net flux of metals out of the marsh, this study also determined the tidal creek water concentrations along with the SF to help understand the contribution from the SF to the creek waters.

1.2 Site Applicability

The site of this study represents a back barrier island marsh free from terrestrial freshwater input, a feature common along the east coast of the United States. In salt marshes, tidal pumping forces oxygenated seawater into the sediments during flooding tides and drains oxygen depleted pore waters into the tidal creek during ebbing tides. The recirculation of seawater through the marsh sediments could represent a significant redistribution agent for metals between the marsh and the coastal ocean, through the tidal creek. Studies which have examined salt marsh systems have primarily investigated groundwater abundances of elements and nearby open waters to determine fluxes (Duncan & Shaw, 2003; Johannesson et al., 2011). These fluxes are primarily driven by

freshwater input which provides a net flux of dissolved metals to the marsh-coastal water system from outside sources. In contrast, this study investigated an isolated system, a barrier island salt marsh with no external groundwater input, to determine whether the exchange of coastal seawater through salt marsh sediments can generate a flux of metals to the coastal water. This exchange is discharged into the tidal creek during the ebbing tide. Monitoring these three hydrologic zones; the SF, tidal creek waters, and coastal waters, will allow us to place tight constraints on the mobility of metals within the system and provide some first estimates of metal fluxes from the salt marsh into the tidal creek/coastal water. Korestsky et al. (2008) & Das et al. (2010) showed that the sediments at the Cabretta site have high concentrations (>10ppm) of absorbed Zn, Fe, Nd, and Pb. The current study shows that the SF in contact with these sediments have significantly higher concentrations (>100x for Mn, Fe, Nd) of metals than surrounding coastal waters. What is unclear is the extent of SF contribution to the nearby waterway via the tidal creek. The SF and the tidal creek have different redox properties, and the migration of metals across this steep redox gradient is hypothesized to control fluxes between these fluids.

1.3 Location

The field site is located on Cabretta Island off the coast of Georgia, southeastern United States. Cabretta is a small island seaward of Sapelo Island, home to the University of Georgia Marine Institute. Most of Sapelo Island is state protected and Cabretta Island itself is uninhabited. This provides a fairly pristine site to conduct the study. Cabretta is a barrier island with a washed over dune and an upland forest. The marsh is located landward of the forest, between Sapelo and Cabretta (figure 1.2 & 1.3).

The location represents an area of marsh which is separate from free flowing freshwater (except rainwater) and is recharged by tidal pumping of seawater. The semidiurnal tides have an average range of 2.5 m and the depth of the creek at the site is about 2 m. (Wilson et al, 2011). This results in nearly complete draining and surface inundation of the marsh twice over a single tidal cycle. This site has been studied extensively for groundwater flow models which have been calibrated using radium data collected from the site by Dr. Wilson's lab. The island is also part of the National Estuarine Research Reserve (NERR) and part of the U.S. Geological Survey's Mercury Deposition Network (MDN).

1.4 Sampling

The sampling regime covered the three basic hydrologic zones of the marsh; the creek which connects the marsh to the coastal waterway, the SF in contact with the marsh sediment and the creek, and the coastal waterway which feeds and receives water from the creek. All three of these zones are influenced by diurnal tidal pumping which effectively controls the hydraulic gradients between open water and subterranean marsh fluids. The tidal creek was sampled hourly over two ebbing tides in order to test for the influence of tidal pumping on metal concentrations due to the hypothesized mixing between SF and coastal water. Using this high temporal resolution, transient metal concentrations in the creek were determined and used to calculate metal fluxes to the creek from the marsh SF. The SF were collected from the bottom and side of the creek using cores at low tide and sampled with high vertical spatial resolution (5 cm) using in situ rhizon samplers. Creek sampling took place around the same point in the tidal cycle over both days to capture the composition of the system within a similar time stamp.

Coastal water was sampled less frequently throughout the tidal cycle as these open waters are expected to be well mixed.

1.5 Elements of Interest

1.5.1 Iron & Manganese

The diurnal cycling of oxygenated and reduced seawater may play an important role in the flux of redox sensitive metals and other elements into and out of the salt marsh. For example, as microbial activity reduces sulfates to sulfides and Fe(III) into the more soluble Fe(II). This, and the low amounts of dissolved oxygen, generally lead to significantly higher Fe concentrations in the marsh pore fluids, while some of that Fe(II) will precipitate as pyrite (FeS) (e.g. Giblin, 1984; Taillefert et al., 2007). As this fluid drains from the marsh into the creek during low tide, the Fe-rich anoxic water will mix with oxygenated coastal water, which in turn is expected to oxidize iron and lead to oxyhydroxide precipitation. So it is unclear the extent to which these high Fe fluids contribute to the dissolved Fe budget of the creek and subsequently to the coastal water. Manganese also forms insoluble oxyhydroxides and sulfides; however, it tends to stay solubilized in the fluid significantly longer than Fe (Beck et al., 2006). The difference between the redox chemistry of these two elements may determine their ability to migrate into and out of the system. Fe, as well as Mn, precipitation has been shown to remove certain elements from solution, especially those which are particle reactive (Lee et. al., 2001). So it is important to study Fe and Mn concentration gradients together with elements that are expected to be particle reactive to test the extent to which Fe precipitation may dominate the cycling of other metals.

1.5.2 Rare Earth Elements

Previous studies (Elderfield & Sholkovitz 1987, Johannesson et al, 2010), have shown REE to be in higher concentrations in shelf pore fluids and tidal creeks over open coastal waters, respectively. Elderfield & Sholkovitz (1987) showed that reduced seawater systems, such as those formed in anoxic benthic sediments, can mobilize REEs. Johannesson et al. (2010) also determined that REE abundances in coastal lagoons (SF and surface waters) can be over 100x greater than offshore coastal waters. Therefore, REEs behave as Fe, high in reduced fluids but low in oxidized fluids, leading to the hypothesis that REEs are being scavenged with Fe-oxyhydroxides during mixing of SF with oxygenated waters. In that case, the fluxes Johannesson et al. (2010) determined, which did not account for REE scavenging, may overestimate REE fluxes to the coastal waters at Cabretta. Cerium is of particular interest as readily oxidizes to the more particle reactive Ce(IV) in oxygenated seawater unlike other REE as evident in the negative cerium anomaly against other REEs in global ocean surface waters (Elderfield & Greaves 1982).

1.5.3 Uranium

In contrast to Fe and Mn, U is insoluble in its reduced form and soluble in its oxidized form. U concentrations are typically high in seawater due to its conservative nature in oxygenated systems. However, U has been shown to be lower in salt marsh creeks than the open ocean (Church et al., 1996). This study showed that salt marsh sediments are a sink for U and suggest that the major mechanism for this removal is reduction of U into its insoluble U(IV) state. Therefore, due to the large concentration contrast of U vs. Mn and Fe between the reduced and oxic waters, these element pairs

should be sensitive tracers of mixing between reduced marsh SF and oxic open coastal waters.

1.5.4 Chalcophile Elements (Cu, Zn, and Pb)

A few studies have examined the interaction of selected chalcophile elements (Cu, Zn, & Pb) within various zones of the marsh (Koretsky et al., 2008; Santos-Echeandía et al., 2010). Koretsky et al. (2008) & Santos-Echeandía et al. (2010) showed that SF in the shallow surface sediments (<50 cm) have highly variable concentrations for these elements. The Koretsky et al. (2008) study further showed high spatial variability in concentration throughout the marsh for these elements attributed to sulfide production, metal reduction by microbial respiration, and oxidation by plant roots. Santos-Echeandía et al. (2006) showed variable trends over a tidal cycle for these elements in the surface sediments, and SF as well. These variances were attributed to a change in equilibrium caused by the metal-poor overlying waters mixing with the SF in the sediments.

1.5.5 Mercury

Previous work at the Sapelo site has shown relatively modest mercury concentrations (>10 ppb) in the sediments. These concentrations appear to increase towards the tidal creek (Das et al., 2012). The sediments near the creek have the highest concentration and possibly the highest exchange rate with the nearby waterway. It was hypothesized, based on isotope composition that the Hg load in these sediments was sourced from the coastal water, implying that the marsh is a sink for total Hg.

1.5.6 Conservative Elements

Barium, strontium, calcium, and magnesium are known to be conservative elements in seawater; their concentrations often coincide with salt content. However, these elements are also affected by geochemical cycling and changes in tidal creek concentrations with the outgoing tide may indicate interactions with subterranean sediments (Moore, 1997). Ba and Sr enter the water through fluid-sediment exchanges. As a result, pore fluids often have higher concentrations than surface water due to their contact with the sediments (Charette & Sholkovitz, 2005). However, both of these studies have been conducted in systems which have fresh groundwater mixing with seawater, so it is unclear to what extent the high Sr and Ba concentrations were due to Sr and Ba flux into the system by fresh water.

2. Method

2.1 Sampling Procedure

Tidal creek and coastal water samples were collected in acid washed 125mL polycarbonate bottles that were preconditioned several time with the ambient water. Immediately afterwards, there waters were subsampled via precleaned rhizon samplers attached to 50 mL syringes (Seeberg-Elverfeldt et al., 2005). The syringes used to collect the fluids were precleaned in an acid bath, as well. Before collection, the tubing and filter were preconditioned by pumping the ambient fluid several times. After collection fluid samples were transferred from syringes into precleaned 125mL polycarbonate bottles with a small volume of distilled hydrochloric acid (6M) to acidify the samples and ensure they were preserved for analysis. SF were collected by extracting shallow cores (50cm) from the creek and sampled by inserting rhizon samplers into predrilled holes along the length of the core. The use of the rhizons is critical in keeping high iron fluids from contact with the air, which could potentially cause precipitation of iron oxyhydroxides. The samples were taken from the field and transported on ice to a clean room in the CEMS lab for analysis. In earlier tests, creek samples were initially brought back to the lab and filtered offsite. Results showed that metal concentrations of samples filtered offsite were much lower than those filtered in the field. This suggested scavenging of metals over time. Therefore, all subsequent samples were filtered in the field. Note that for the rest of the discussion, the concentration of metals in the fluids reflects the

"dissolved" fraction, which here is operationally defined as <0.15 microns, the exclusion size of the rhizons.

2.2 Method Development

A large portion of this research was to refine the method set forward by Milne et al. (2009) for the determination of Fe, Cu, Pb, Ni, Cd, and Zn in seawater samples to include REEs. The first round of tests were processed using bulk extraction, this varied from the Milne method which uses a column to extract samples. The initial attempt at bulk extraction was problematic due to high and inconsistent blanks. This was coupled with inconsistent yields for the spikes between samples. Eventually the bulk method was dropped for a column extraction. Several tests were conducted with the column extraction to determine yields, fractionation, and to validate the method. Throughout the tests, issues became apparent with the column method. Rare earth elements were not making it onto the column during extraction and the REE spike was not recovered. The column method worked for the other spiked elements but not the REEs. Problems were also seen in Pb, which was determined to be a contamination issue. It was determined that many of the problems with the method development stemmed from ineffective cleaning of the resin and incomplete conditioning prior to sample loading. Tests showed that the resin needed extensive rounds of cleaning with 1M nitric acid (HNO_3) to reach background levels (>100 acid to resin volume ratio). Eventually the column extraction was replaced by a refined bulk extraction method. In the column method, samples were buffered before entering the column. It was hypothesized that high iron samples could precipitate Fe during buffering to pH 6, and scavenge the REEs, which react with iron hydroxides at natural pH ranges. In the refined bulk extraction method, the resin is added to the sample

prior to buffering. This new method had increased yields and precision for the REEs and we hypothesized that the resin addition prior to buffering to pH~6 may have allowed the REE to bind to the resin before the hydroxides formed. This bulk extraction method was tested, validated, and used to process the final round of samples. Some yield problems were still encountered on SF, which we attributed to very high organic load that was not removed by the ultraviolet (UV) light + hydrogen peroxide (H_2O_2) treatment.

Initially, a multi-REE spike containing an enriched isotopic composition of ^{145}Nd, ^{149}Sm, ^{155}Gd, ^{161}Dy, and ^{171}Yb was used. However, tests showed that REE do not fractionate during extraction (figure 2.2). Using this information, the multi-REE spike was replaced by a single element ^{145}Nd spike. Neodymium concentrations were determined by isotope dilution based on the known isotopic composition of the spike using the isotope dilution (ID) equation below:

$$[\mathrm{Nd}]\mathrm{sample} = \frac{\left(\frac{^{145}\mathrm{Nd}}{^{146}\mathrm{Nd}}\mathrm{measured} - \frac{^{145}\mathrm{Nd}}{^{146}\mathrm{Nd}}\mathrm{spike}\right)}{\left(\frac{^{145}\mathrm{Nd}}{^{146}\mathrm{Nd}}\mathrm{natural} - \frac{^{145}\mathrm{Nd}}{^{146}\mathrm{Nd}}\mathrm{measured}\right)} \cdot \frac{(\mathrm{AtWtNdNatural} \cdot \mathrm{SpikeMass})}{(\mathrm{AtWtNdSpike} \cdot \mathrm{SampleMass})} \cdot \frac{[\mathrm{Nd}]\mathrm{Spike} \cdot {}^{145}\mathrm{NdSpike}}{^{146}\mathrm{NdNatural}}$$

Rare earth element concentrations were calculated from a 1 ppb REE standard that was extracted together with the samples, using the Nd concentration in the sample determined by isotope dilution as an internal standard. Using this precise concentration of Nd, and comparing the sample to the extracted pattern of a solution with known REE concentration, the other elements can be calculated from Nd. To do so, the mass of the spike is removed from the measured signal of the sample and compared to the extracted standard.

The concentration of the other elements was determined by the equations below:

$$\mathrm{cps}^{146}\mathrm{Ndsample} = \mathrm{cps}^{146}\mathrm{Ndmeasured} \cdot \frac{\frac{\mathrm{SampleMass} \cdot [\mathrm{Nd}]\mathrm{Sample}}{\mathrm{AtWtNdNatural} \cdot {}^{146}\mathrm{NdNatural}}}{\frac{\mathrm{SampleMass} \cdot [\mathrm{Nd}]\mathrm{Sample}}{\mathrm{AtWtNdNatural} \cdot {}^{146}\mathrm{NdNatural}} + \frac{\mathrm{SpikeMass} \cdot [\mathrm{Nd}]\mathrm{Spike}}{\mathrm{AtWtNdSpike} \cdot {}^{146}\mathrm{NdSpike}}}$$

$$[\mathrm{REE}]\mathrm{sample} = \mathrm{cpsREEsample} \cdot \frac{[\mathrm{Nd}]\mathrm{sample}}{\mathrm{cps}^{146}\mathrm{Ndsample}} \cdot \frac{\mathrm{cps}^{146}\mathrm{Ndstandard}}{\mathrm{cpsREEstandard}}$$

The concentrations of the standard are uniform for every rare earth element so there is no change in the abundance of Nd and the target element. If the standard has difference abundances between elements, this must be accounted for in the calculation. In this equation, that correction is 1, and therefore not shown.

The advantage of this method is the explicit and accurate determination of a single REE by ID while the other REEs are effectively “anchored” to that element. Other methods (Freslon et al., 2011) have sacrificed a single REE, like Tm, in the sample by overwhelming the sample with a known concentration of the element. Then by using the known concentration of the enriched element, they determine other REEs by comparison to a standard solution. This method allows for the determination of all the REEs without sacrificing any in the process along with improved precision on the spiked element.

In addition to isotope dilution and external calibration, oxide formation correction was necessary to provide accurate determination of several elements of interest. Molybdenum causes oxide interferences on Cd isotopes and was corrected for in Milne et

al (2009). In this method, further steps were implemented to ensure accurate measurements beyond Mo/Cd. Measuring the rare earth elements in low resolution mode ($\Delta M/M=300$) on the ELEMENT2 allows for determination of elements at lower concentrations as compared to high resolution. However, it makes it impossible to separate interfering oxides from the isotopes being measured. The REE are particularly problematic because oxides from light mass REE (e.g. ^{139}La) appear on the middle mass REE (e.g. $^{139}La^{16}O$ on ^{155}Gd) while middle mass REE oxides appear on heavy mass REE. In order to correct for this, tests were conducted to determine oxide formation for each element. Figure 2.3 shows the variability of oxide formation for different REEs. The lighter REEs create oxides more readily, with La being the highest. The oxide formation is also linear across a large range of UO/U oxide formation. In order to correct the samples, the regression results of these lines were applied to each interfering and interfered isotope as a function of UO/U measured in each sample to determine the absolute value of oxide formation for each element. The advantage of U is that it is always available in these types of samples, and allows for an internal oxide formation monitor for every sample. Samples and standards with low uranium however, require additional uranium to better track the oxides.

Barium, molybdenum, and zirconium oxides were also measured because of their interferences with elements of interest. We also found that the Toyopearl resin has a high Zr blank and Zr oxidizes more than Mo, so it was necessary to monitor and correct for both to determine Cd. Regression values for elements of interest are listed in table 2.1. These values were used to determine oxide formation on isotopes of higher mass, La -> Gd for example. However, tests showed that these oxides also have to be added back onto

their original isotope. Based on figure 2.4, it is necessary to not only subtract the oxide from the isotope which is interfered but also to add the oxide back onto the original isotope. This is shown in the equations below:

$$^{155}Gd_{true} = {}^{155}Gd_{measured} - {}^{155}LaO$$

$$^{139}La_{true} = {}^{139}La_{measured} + {}^{155}LaO$$

where $^{155}LaO = f(UO/U)$

These corrections become important if there is a large difference in oxide formation between samples and standards. Therefore, this correction has to be made both to the samples and the calibration standard.

REE recovery was tested using two separate standards. 50 ug of the USGS reference material BIR-1 (a basalt rock) was extracted (table 2.3). Also, to match the salt matrix found in samples, 30 g of a seawater standard was extracted (figure 2.5). Both samples were within 10% of all reported values with the exception of cerium for the seawater sample. This sample was processed in four replicates and all replicates gave similar values, higher than the reported Ce, suggesting the standard may be contaminated.

2.3 Sample Analysis and Extraction Method Outline

The major cations in seawater Mg, Ca, Sr, Ba, Mn, U, as well as Fe for high iron samples, were determined by dilution on an ELEMENT 2 High Resolution Inductively Coupled Plasma Mass Spectrometer (HR-ICPMS). The samples were diluted in distilled 2% HNO_3 with 1 ppb indium to correct for signal suppression and drift due to matrix effects. The samples were run against a well-known rock standard to determine element concentrations.

Other elements, and Fe in low iron samples, were determined by bulk extraction and ID adapted from Milne et al. (2009). Samples were added to acid refluxed 30 mL PFA Teflon bottles. Sample extraction masses ranged from 5g for SF to 20g for coastal waters. In order to overcome issues with extraction yields and elemental fractionation on the resin, samples were spiked with an enriched isotope composition of ^{57}Fe, ^{65}Cu, ^{62}Ni, ^{68}Zn, ^{111}Cd, and ^{207}Pb isotopes using an aliquot of the spike from the Milne method, and an enriched isotope spike for ^{145}Nd was added for the REEs. Hydrogen peroxide was added drop-wise to the spiked samples. The samples were capped and irradiated in the PFA bottles under UV light for several hours, in a homemade UV box. This step helps breakdown organic compounds in the samples which can compete with the resin during the extraction (Milne et al. 2010).

Once irradiated, 100 uL of Toyopearl AF Chelate 650, an iminodiacetic acid (IDA) resin, was added to each sample bottle. The Toyopearl resin extraction removes the matrix (Na, Mg, and Ca) and effectively concentrates the analytes of interest. The extraction is sensitive to pH, so the pH of samples was adjusted (pH≈6) using an ammonium acetate buffer (3M). The pH of each sample was measured precisely using a pH microprobe on small aliquots of the buffered sample. Buffered samples were placed on a shaking table for several hours to complete extraction. After shaking, the remaining supernatant was decanted from the resin. The resin was transferred to acid washed 2 mL centrifuge tube for rinsing and final elution. The resin was rinsed using 2 mL of 18mΩ SuperQ water which is slightly buffered using ammonium acetate (0.1M) to prevent early elution of elements from the resin while removing the residual salts from the resin prior to final extraction. The rinse solution is pipetted off and the resin is eluted using 1 mL of

distilled HNO_3 (1M). The elution acid is isolated from the resin and transferred to a 4 mL acid washed vial for determination on the ICPMS. Blanks were processed the same as the samples, by using smaller volumes of spike in 1 mL 18mΩ SuperQ water. Several blanks were processed to track consistency of the blank. The blanks were then subtracted from the samples. Processing schematic found in figure 2.6.

The element cuts from the extraction method were run on the ELEMENT 2 HR-ICPMS. The REEs, Cd, and Pb were measured in low resolution, while the other TMs were measured in medium resolution to resolve isobaric interferences. Magnesium was also measured in medium resolution to monitor salt load on the system. A cyclonic spray chamber, 100 μL flow rate probe, and Teflon nebulizer setup was used to maintain steady flow and ensure enough sample was delivered for measurement. The instrument was optimized for high sensitivity and low oxide formation. A multi-REE solution was extracted and run during the analysis to measure the extraction fractionation and mass bias of the instrument. These measurements were used to determine unspiked REEs.

3. Results

3.1 Manganese

Coastal waters enter the Cabretta marsh during flooding tides and marsh fluids are exported to the coastal ocean during ebb tides. Net processes between these two end-members are integrated in the tidal creek over the turning tides. Ebb tide concentrations of manganese, for example, are much higher than surrounding coastal seawater (20 ppb vs. 5 ppb) but lower than SF in close proximity to the creek (738 ppb vs. 469 ppb) (figure 3.1). This trend is observed over both days with similar magnitude between the two days. Importantly, the Mn concentrations in the tidal creek show a regular increase with time (i.e. with ebbing tide), with lowest concentrations, close to coastal waters, observed during high tide and highest during low ebb tide with concentrations closest to the SF end-member. This qualitatively suggests increasing addition and export of SF into the creek with ebb tide. It is important to note that persistent high Mn concentrations in the creek suggest slow oxidation of Mn, at least during the time scales and sampling of this study.

3.2 Uranium

The U concentration in the SF is 5-10 times lower than that of the coastal water. This is supported by the reduction of U to the insoluble U(IV) in the anoxic SF. The U concentrations in the creek waters fall between the coastal and SF, and decrease with decreasing tide for the first ebbing tide. This again suggests fluid export to the creek with low U. The second ebb tide has less variable U concentrations than the first with a slight

increase with time. In both cases, the concentration of the creek is always lower than the coastal water, suggesting dilution of the creek waters by SF export.

3.3 Conservative Elements

Magnesium and calcium concentrations show small variations (~25%) in the tidal creek. Creek water concentrations are both higher and lower than the coastal water for both elements, with no obvious trend over the tide. For Mg, the SF have lower concentrations than most of the creek samples. While for Ca, the concentrations are similar for the two end-members. As Mg and Ca are conservative tracers of seawater, this could be explained by a fresh water component coming from the marsh (there was extensive rainfall during the days leading up to sampling). In that case, we would expect a similar dilution effect for both Mg and Ca, which is not observed. Alternatively, Mg and Ca also become increasingly particle reactive at ph>7 (Sverjensky et al., 2006). Experimental data on quartz in NaCl solutions shows greater adsorption of Mg than Ca between pH 7 and 8 (up to 30 and 10% respectively), qualitatively consistent with the behavior of these elements in the SF in the dominantly quartz sandy soils of the marsh (Das et al., 2013).

3.4 Iron and Rare Earth Elements

Iron and REE (using Nd as a proxy) are low in the coastal water (1ppb and 10ppb respectively) and variable but up to 2-3 orders of magnitude higher in the SF. Fe and REE concentrations both vary an order of magnitude between the two ebb tides in the tidal creek and do not correlate well with tidal height. This non-conservative mixing behavior of Fe is qualitatively consistent with rapid oxidation of Fe(II) to Fe(III) and precipitation, as SF enters the creek and mixes with oxygenated water. The close

correlation of REE with Fe concentrations is then consistent with their highly particle reactive behavior, where they may become scavenged out with Fe precipitation. In either case however, SF seem to export REE and Fe into the creek waters, albeit in highly variable amounts.

3.5 Rare Earth Element Patterns

Rare earth element patterns in the SF are highly variable ranging from near coastal water composition to highly light REE enriched (figure 3.5). Despite the variability in the SF, the creek patterns are consistent across the ebb tide with slight variations (32% overall for La) in concentrations. All the creek water patterns have a positive cerium anomaly which is not seen in the coastal water. All of the creek patterns flatten out towards the heavy REE. There are also positive excursions on Sm and Eu for all of the creek waters. These anomalies appears in a few of the SF end members as well.

3.5 Chalcophile & Siderophile Elements (Cu, Ni, Zn, and Pb)

Copper, Ni, and Zn behave similarly in the creek changing little between the two ebbing tides. The end-member composition of these elements varies slightly with Ni and Zn having higher concentrations in SF than coastal water, while Cu end-members on the other hand have similar concentrations. This limited variability between end-members makes it difficult to determine any mixing relationship between coastal water and SF in the creek. Lead, in contrast, behaves different in that it is higher in the SF than coastal water, and there are two separate trends between the two ebbing tides, as seen in Fe and REE. This implies a closer geochemical behavior with REE and Fe than with other chalcophile elements.

3.6 Mercury

Mercury concentrations in the salt marsh fluids are very low. Tidal creek concentrations ranged from 0.5 ppt to 3.25 ppt. Most of the tidal creek samples were near the coastal water concentrations (1.1 ppt) while the SF had slight higher concentration (2.32 ppt). Most samples were measured in duplicates with high variability between duplicates. The low samples were near the detection limit (10pg) and below the calibration curve (15 pg). Due to these overall low Hg concentrations, the patterns for Hg are currently unclear. Nevertheless, we do not observe significantly higher concentrations in the fluids than coastal waters.

4. Discussion

4.1 Mixing Between Coastal Water and SF

The distribution of Mn in the salt marsh is strongly correlated with tidal height and varies between the coastal water and SF end-member composition. This points towards mixing between these two separate sources. In the following, we model the mixing between these two end-members in order to put some quantitative constraints on elemental fluxes from the marsh to the coastal water through the studied creek zone during the ebbing tide. Explicit in our models, is the choice of an "average" SF composition despite the observed variability.

4.1.1 Manganese and Uranium

Manganese and U tidal creek concentrations fall broadly along a mixing line between average SF and coastal water end-members. Mn in the SF is higher than the coastal water while U in the SF is lower than the coastal ocean, but most of variability in the creek is a result of Mn (figure 4.1). The U concentrations in the creek do not correlate as well with tidal height as Mn. This noise may be attributed to U oxidation of suspended marsh sediments which release U into the water. Mn on the other hand, has an apparent slow oxidation in the tidal creek. Based on the above, we suggest that Mn is a good proxy for modeling mixing between coastal waters and SF.

4.1.2 Iron and Rare Earth Elements

Iron and Nd (as a proxy for the rest of the REE) concentrations in the tidal creek show a positive correlation. However, the high variability in the Fe contents of SF makes it difficult to use to an average composition to model Fe/Nd variability for both ebb tides (figure 4.3). The high Fe-Nd tidal creek concentrations for the first ebb tide require a SF end-member with higher Fe and REE concentrations than what was measured in the fluids. It is quite possible that SF compositions variability was not sampled in its entirety, at least for Fe and REE. Alternatively, part of the Fe-REE variability in the tidal creek and perhaps SF, may be due to fast oxidation and subsequent removal of iron in the fluids which will effectively move the tidal creek compositions off the mixing line, in which case conservative binary mixing between coastal water and SF cannot describe the Fe-Nd distribution in the creek.

4.2 Modeling Mixing

As discussed earlier, the large difference in Mn concentrations between the SF and coastal water end-members and the reciprocal tidal creek variability suggest that Mn can be used as a proxy to model mixing. The different Mn concentrations between the SF and coastal water also allow for an evaluation of mixing. This is seen in table 4.1, where SF contribution in the tidal creek is modeled for every creek sample, assuming conservative binary mixing between the average measured coastal water and the average SF. Errors on the estimate of SF component in the creek are estimated using 1 standard deviation of the variance in the SF. The modeling shows that the SF component in the creek water correlates with tide height, consistent with increasing SF contribution to the creek during the ebbing tides.

This mixing model shows ~6% of the SF component present in the tidal creek waters at high tide and ~37% during low tide for the first ebb tide. These values vary between the two ebb tides with only ~1% of the SF in the creek water at high tide for the second day but, the trend is the same. These estimates of SF contribution to the tidal creek also allow us to constrain groundwater discharge from the marsh over the ebb tide, which will be further discussed later. The large estimated errors are due to the large variability in Mn in the SF end-member and our assumption that the SF end-members is the average fluid. Additional SF data may have decreased this variance.

This mixing model can be checked against other elements by mixing average end-member compositions in the same estimated proportions as determined by Mn. Modeled and measured Ni and U show some deviations from the 1:1 mixing with U having the most deviation during the first ebbing tide (figure 4.7). However, all of the predicted values are well within 40% of the measured values. Given the variability of SF composition for these two elements (>170% for U, and >130% for Ni), the precision of this model using only the average composition is considered to be quite good, and could be improved if we were to arbitrarily pick a SF end-member composition from within the observed variability and optimize it to the best fit of the measured creek waters. The fact that Ni shows a correlation with Mn, suggests that there are similar processes involved in their export to the tidal creek.

4.2.1 Groundwater Discharge Estimates

As shown above, Mn is a good indicator of mixing between the average coastal water and SF end-members, and can be used to constrain the amount of SF in the creek. Concentrations of the end-members used for estimating discharge are listed in table 4.1.

Using the modeled SF % contributions to the creek waters shown in table 4.2, we can estimate an ebb tide discharge for the two days. Discharge was estimated using the below equation:

SF Discharge (L/m^2/ebb tide) =Σ ($\%SF_n$ * TH_n – ($\%SF_{(n-1)}$ * $TH_{(n-1)}$ - $\%SF_{(n-1)}$ * TH_n)); Where % SF is modeled SF composition of the creek, and TH is tide height, n is the sample.

Based on these calculations, the SF discharge ranges from 1140 +/- 557 L/m^2 – 544 +/- 266 L/m^2 per ebb tide respectively, where discharge is normalized to the creek water surface area, m^2. These rates are highest during the mid-tides (283 L/m^2/hr) and lowest at high and low tides (143L/m^2/hr - 40L/m^2/hr respectively). The variations on the average discharge are the calculated errors for the %SF calculated in the creek shown in table 4.2. The contribution of the SF to the tidal creek is determined by Mn concentration in the creek. Any oxidation of Mn which occurs during export will remove Mn from the observed creek water concentrations. Therefore, these estimates are minimum contributions and may be higher if Mn is precipitated once SF enters the creek. Based on estimates of creek volumes, this represents somewhere between 11 – 32% of the total volume of water in the creek at high tide.

4.3 Estimating Fluxes

The primary goal of this study was to constrain fluxes from the salt marsh into the tidal creek. The mixing model presented above helps to understand end member compositions in the creek, and equally important, deviations from additive mixing of

known end members. Fluxes between SF and the tidal creek were determined by the difference in the tidal creek water concentration from the initial coastal water end member composition. The explicit assumption is that for a fully conservative element the concentration during ebb tide should be equal to the concentration during flooding tide and equal to the local coastal water (i.e. no change). Instead, if the ebb tide has higher (lower) concentration than the coastal water, then the marsh would be a source (sink) for that particular element. The export from the marsh over an ebb tide then is calculated by the simplified equations using measured concentrations:

$$Creek_{out} = SW_{in} + Marsh_{out}$$

$$Marsh_{out} = Creek_{out} - SW_{in}$$

Where the $Creek_{out}$ is the flux into the creek, $Marsh_{out}$ is the flux from the SF, and the SW_{in} is the flux into the marsh from the coastal seawater. Assuming conservative addition of coastal water into the marsh during flooding tide, the difference between the concentrations of incoming coastal water and outgoing tidal creek is the contribution from the marsh. Fluxes for elements from the marsh were calculated using the equation below:

$$([\ ]_{sw} - [\ ]_{creek})_{avg} \cdot (\text{High Tide (m)} - \text{Low Tide (m)}) \cdot 1\text{m Width} \cdot 1\text{m Length}$$

$$= g \cdot m^{-2}/\text{ebb tide}^*$$

*Values are creek water surface normalized

Concentrations are in g/m^3 using density of $1024 kg/m^3$ for seawater

The fluxes from the marsh into the creek are listed in table 4.3 & 4.4. The data shows a negative flux for U into the creek and supports the marsh as a sink for U,

consistent with studies at similar marsh sites (Church et al., 1996; Duncan & Shaw, 2003). But here we demonstrate that U uptake takes place in salt water systems as well. Fluxes for other metals (Mn, Fe, & Ni) are positive but their relative fluxes are very different. Manganese has close to 10x more export than Fe from the marsh, despite having similar concentrations in the SF. Sulfur has a negative flux from the marsh, which could be attributed to sulfide formation (e.g. Koretsky et al., 2008). However, the lack of correlation between S and Cu, Zn, Pb concentrations suggests limited effect of sulfide precipitation on the chalcophile elements. A negative flux for several conservative elements (Ca, Mg, and Sr) points to a sink in the marsh, perhaps due to adsorption. However, the tidal creek concentrations are very close to coastal water concentrations and the fluxes for these elements are small compared to their abundance in the coastal waters, and likely insignificant. Fluxes for the REE are similar with the exception of La and Ce. There is an excess Ce export for the first day shown by the REE patterns in the creek. This may be attributed to a high Ce SF component, consistent with reduced fluids. The lack of a Ce anomaly on the measured coastal water, which is the assumed initial fluid, may also under-predict the Ce export from the system. Cerium in the surface ocean is high (1.4ppt) and sharply decreases with depth. However, the coastal water at Cabretta has 10x more Ce than reported open ocean values (Pahnke et al., 2012), consistent with the Ce export into the open water. High Ce export relative to other REE has also been seen in similar systems by Johannesson et al. (2011). The magnitude of the REE fluxes in our study are lower than those reported by Johannesson et al. (2011) which may be attributed to the difference in location between our salt water system and the fresh water source in that study.

5. Conclusion

The analytical method developed for this study is robust for determining open ocean and coastal waters for rare earth elements in addition to several transition metals (Fe, Ni, Cu, Cd, Zn, and Pb). The rare earth elements are determined by a combined isotope dilution and external calibration. The REE and transition metals can be determined in 30mL of sample or less depending on sample composition. The method has a low blank (in the low pg range for REE) and samples can be quickly processed without need for a complicated plumbing system. The bulk extraction further allows for a large number of samples to be processed simultaneously. Correction of the oxides is important to minimize the effect of oxide formation in the plasma on the elemental concentrations as both an addition to and suppression of the signal for elements of interest. This method was adopted for use in the Cabretta salt marsh as a case study.

Salt marsh tidal creeks connect subterranean marsh fluids with the coastal ocean. This study examined changes in the tidal creek water composition over an ebbing tide to constrain mixing of SF and coastal waters. Concentrations of certain elements (Mn, U, S, and Ni) in the tidal creek waters vary as a function of both tide height and concentration difference in between coastal waters and SF. These elements can be used to model mixing between the average coastal water and SF end-member compositions as shown with Mn/U. Estimates based on Mn concentrations show that the SF contribution to the creek waters varies with tide height ranging from ~6% at high tide to ~37% at low tide. This contribution results in an average export of 842L/m^2 of SF from the marsh on an ebb tide, and represents 11 - 32% of the total volume of water in the creek at high tide.

The elemental fluxes from the marsh are consistent with studies from similar sites, showing the marsh as a source of Mn and Fe and a sink for U and S. The marsh is also a source for dissolved REE, with excess Ce, which has also been seen in other studies with terrestrial freshwater mixing with submarine groundwater (Duncan & Shaw, 2003; Johannesson et al., 2011). The recirculation of coastal water with marsh sediments creates redox gradients which provide mechanisms for metal mobilization and sequestration. These salt marshes as transient shoreline features are now shown to export metals from their sediments into nearby waterways. There may also be additional seasonal variability with these fluxes, but this study has provided a benchmark for further investigation.

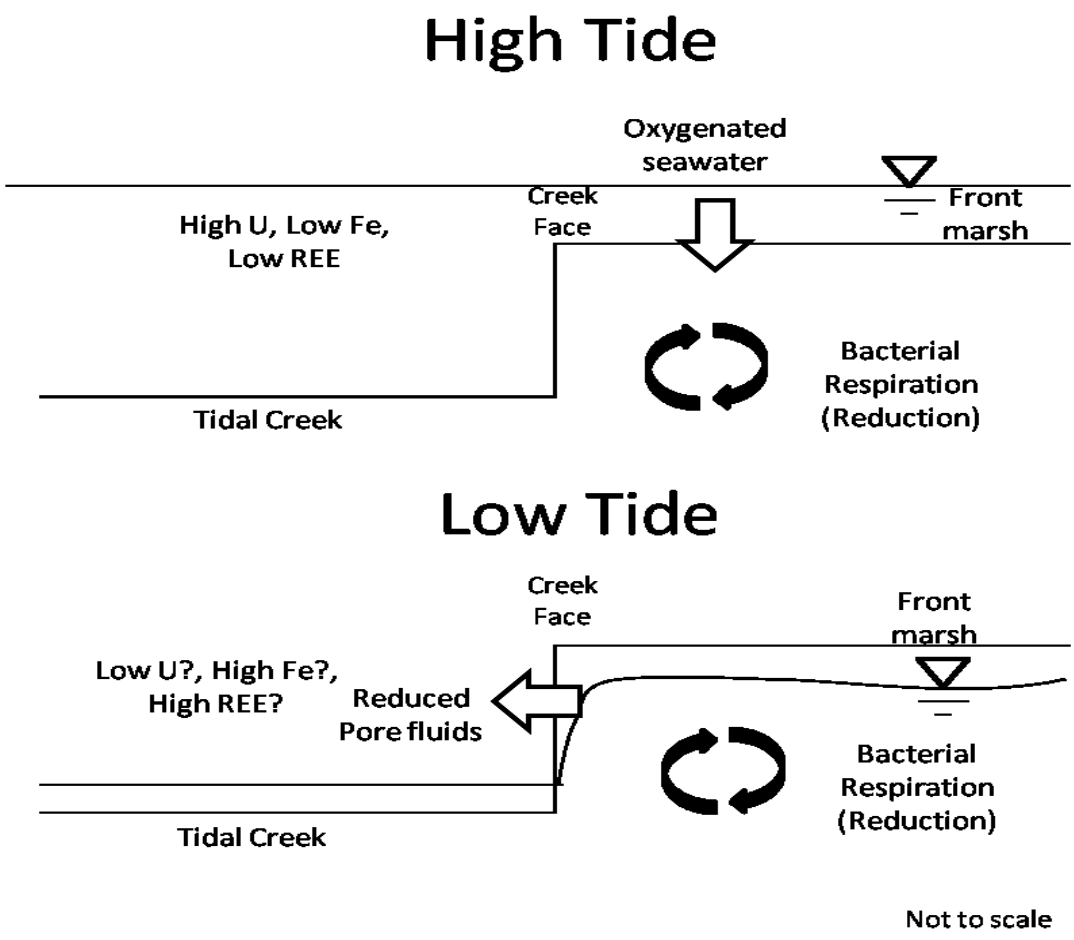

Figure 1.1 Schematic of tidal pumping across the creek face at high (top) and low (bottom) tide.

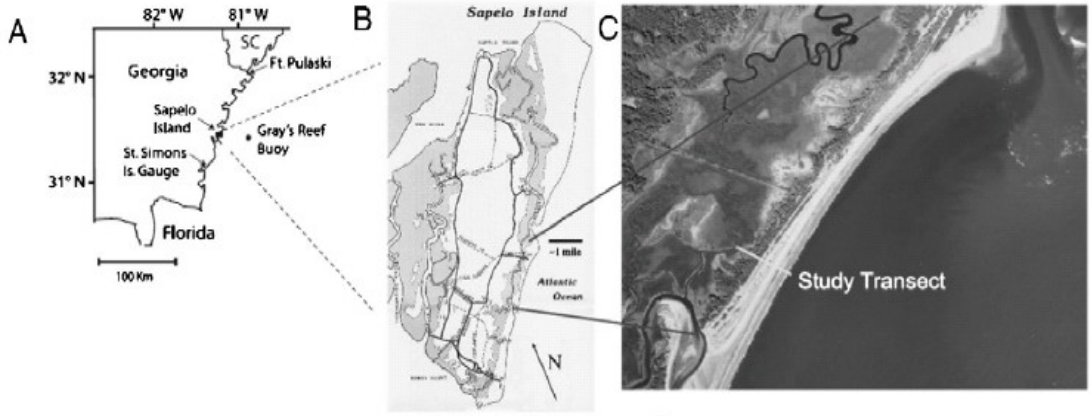

Figure 1.2 Map of study site. A. Georgia coastline, B. Sapelo Island, C. Cabretta Island with transect location for this study.

Figure 1.3 Cabretta Creek near low tide. Face of the creek is exposed and cord grasses line the banks. View is approximately SSW.

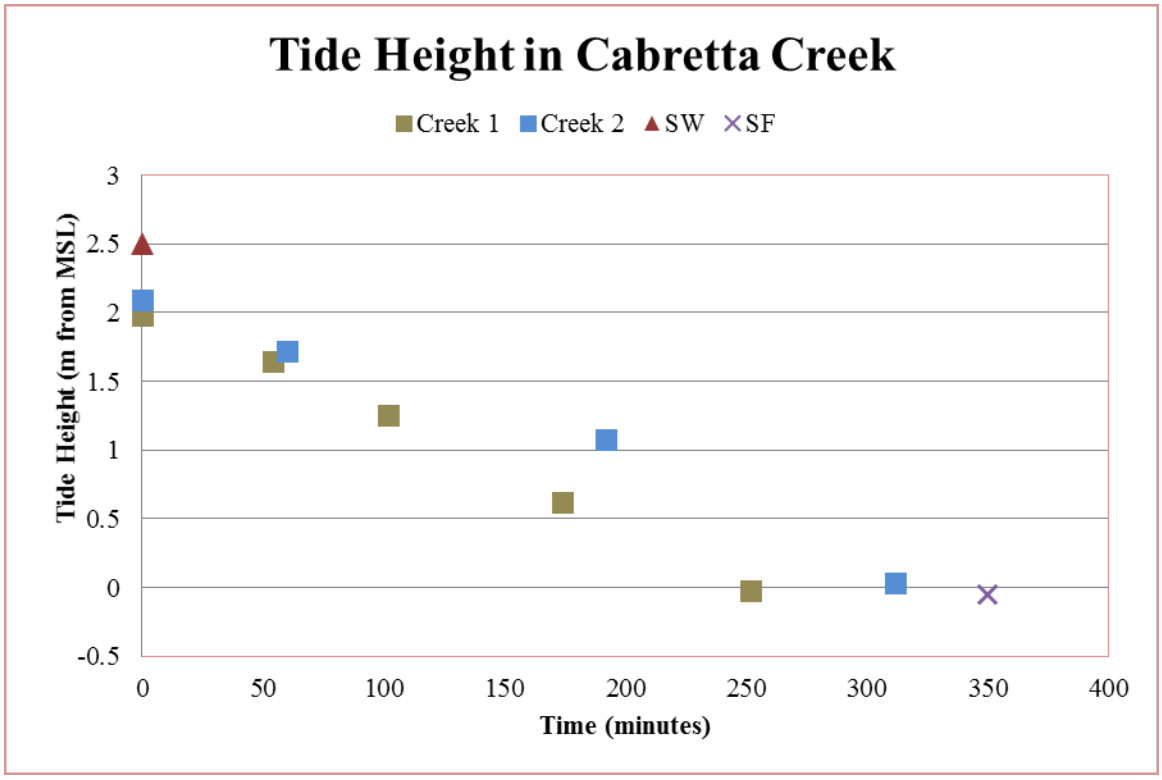

Figure 1.4 Tide height (relative to mean sea level) over the two ebbing tides. Creek 1 & 2 refers to which sampling day they were collected. Ocean and subterranean fluids are anchored to show highest and lowest point measured.

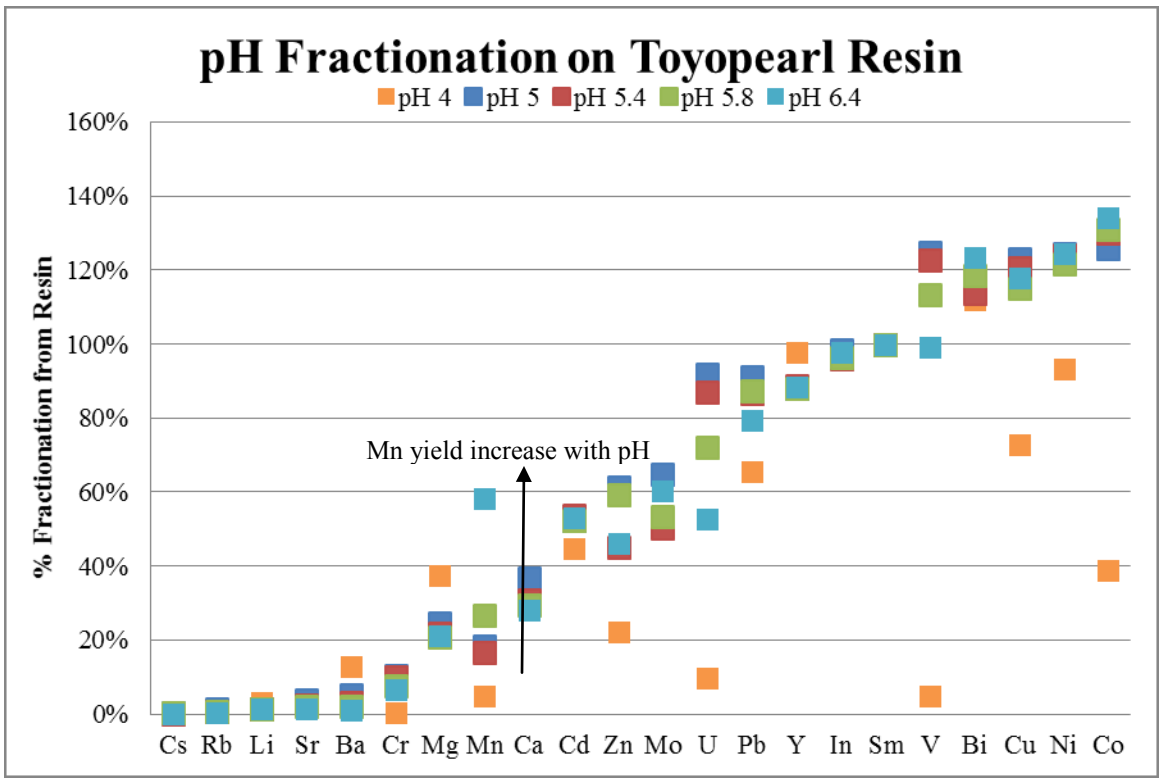

Figure 2.1 Resin fractionation as a function of pH, normalized to Sm. Low pH threshold for multiple elements (Zn, U, V, Cu, Ni, Co). Others are consistent across broad pH ranges. Large variability for Mn and U.

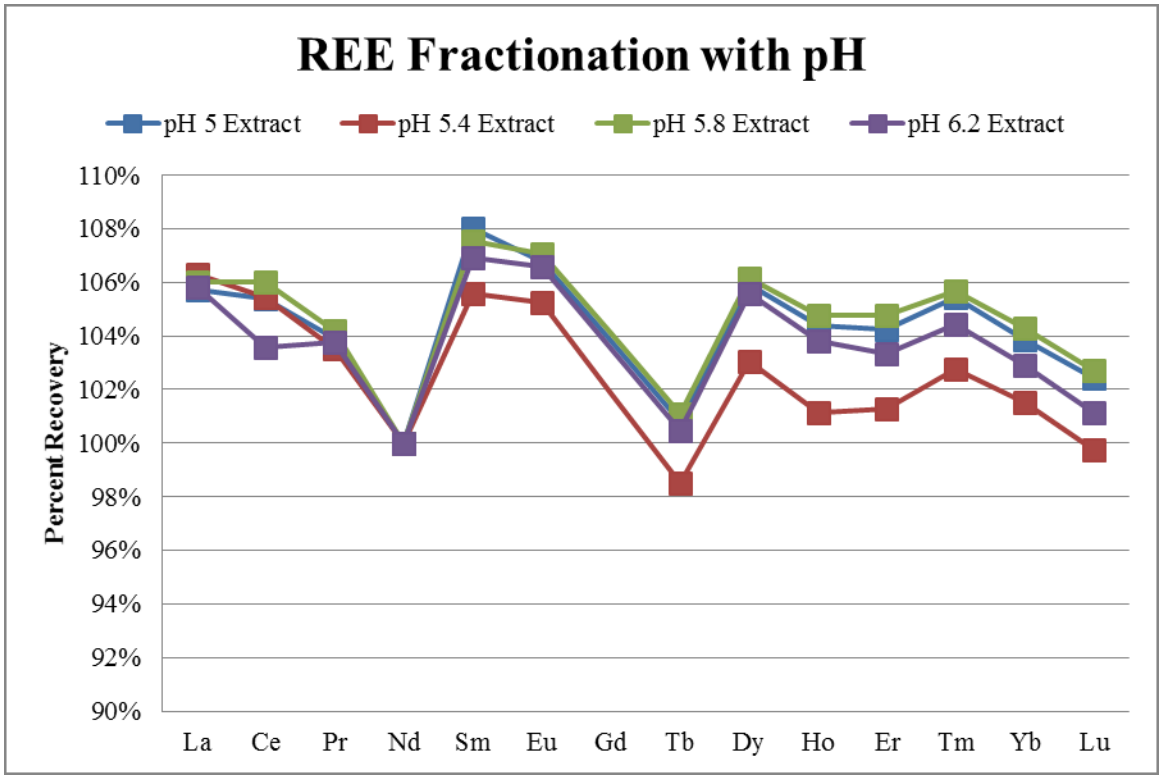

Figure 2.2 Rare earth element fractionation over pH ranges, variability less than 5% for all elements.

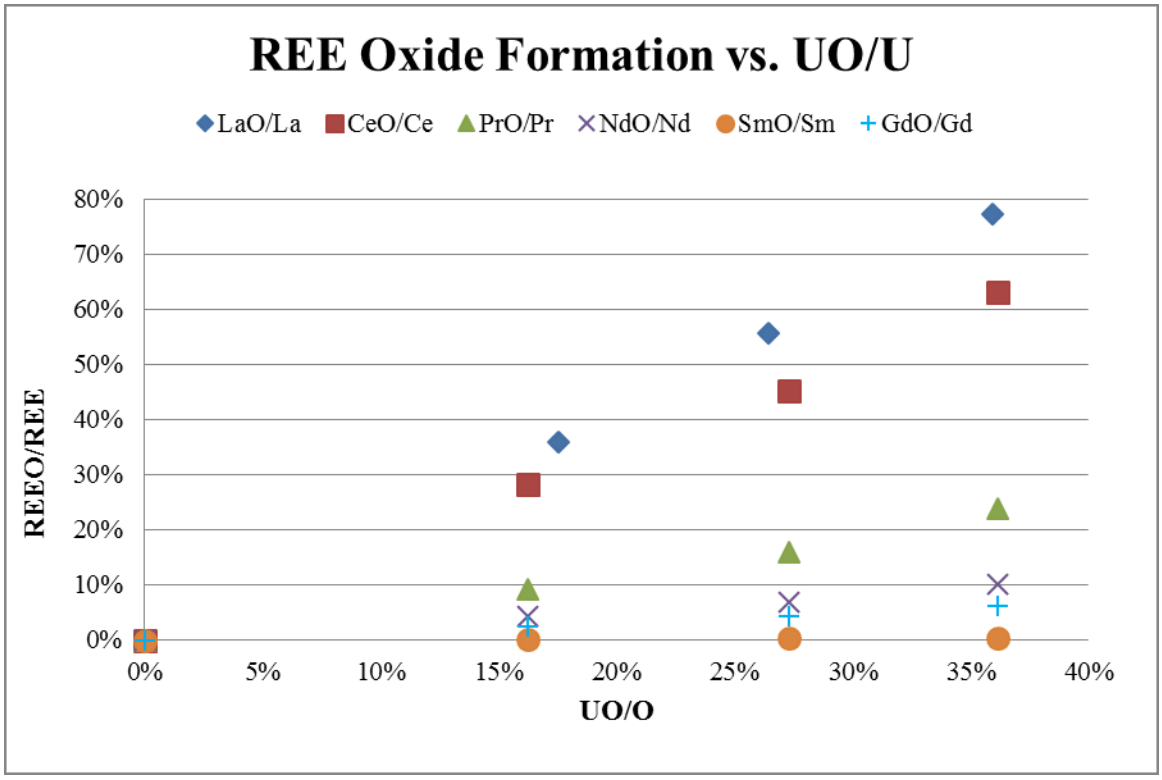

Figure 2.3 Oxide formation for various REE as a function of uranium oxide.

Table 2.1 Oixide Formation Regression as a function of UO/U

	Slope	Intercept	Rsq
LaO/La	2.434	-0.049	99.97%
CeO/Ce	1.962	-0.043	100.00%
PrO/Pr	0.693	-0.019	99.87%
NdO/Nd	0.265	0.000	99.78%
SmO/Sm	0.005	0.002	99.78%
GdO/Gd	0.152	0.000	99.79%
BaO/Ba	0.003	0.001	99.99%

Slopes and intercepts of oxide formation as a function of UO/O formation. These values determined with 100uL flow rate probe, Teflon nebulizer, & glass cyclonic spray chamber. These values vary based on setup, but remained consistent stable between runs.

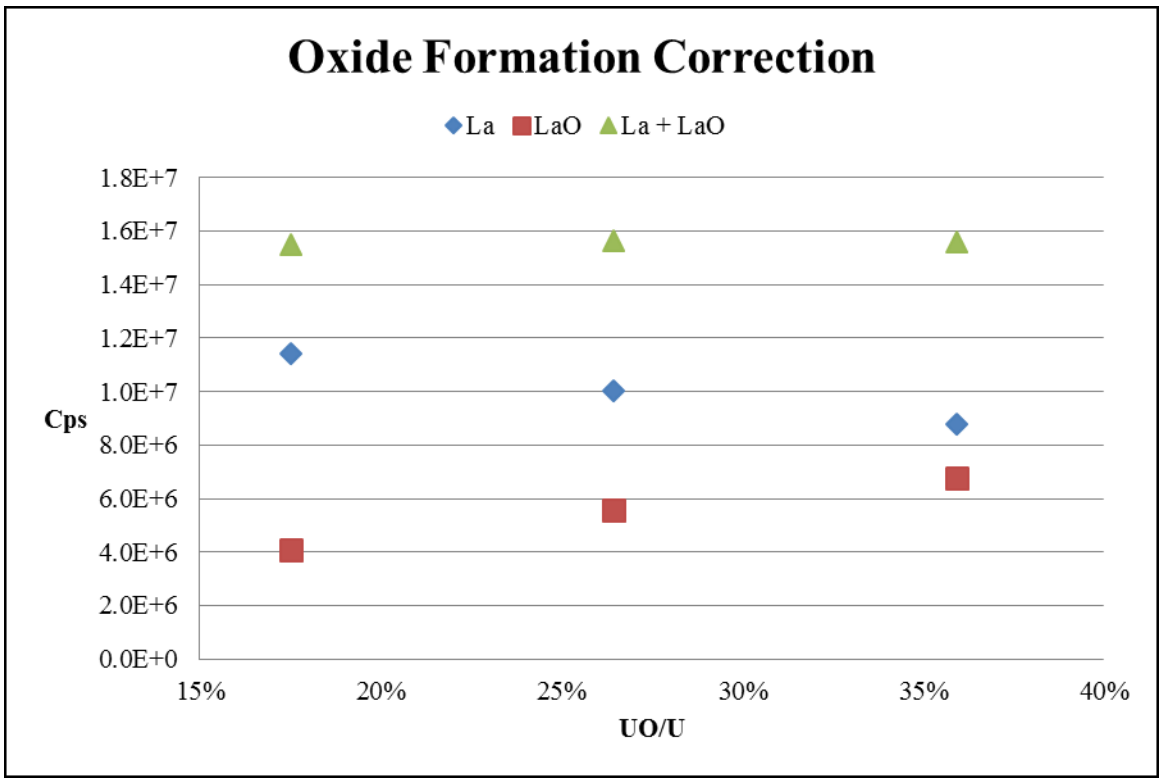

Figure 2.4 La & LaO signal as a function of UO/O formation. Increasing oxide creates apparent suppression of La signal. However, adding the oxide back to La produces a consistent signal across a wide range of oxide formation.

Table 2.2 Rock Standard BIR recovery

	Analyte Processed (pg)	Measured (pg)	% Recovered	Blank %
La	30.75	33.7	109.60%	1.80%
Ce	96	93.71	97.60%	1.05%
Pr	18.5	17.82	96.30%	0.70%
Nd	119	117.67	98.88%	2.20%
Sm	56	53.99	96.40%	0.23%
Eu	26.5	25.61	96.60%	0.18%
Gd	93.5	97.16	103.90%	0.18%
Tb	18	17.53	97.40%	0.17%
Dy	125.5	126.11	100.50%	0.05%
Ho	28	28.63	102.20%	0.06%
Er	83	85.58	103.10%	0.04%
Tm	12.5	11.96	95.70%	0.14%
Yb	82.5	77.9	94.40%	0.05%
Lu	12.5	12.8	102.40%	0.14%

Percent recovery of rock standard BIR (50ug). Small deviation between elements but all within 10% of reported values.

Table 2.3 CASS-5 Reference Material

	Measured (ug/kg)	+/-	Reference (ug/kg)	+/-
Cd	0.024	0.003	0.021	0.0017
Pb	0.013	0.003	0.011	0.002
Fe(*)	4.348	0.309	1.4	0.11
Ni	0.259	0.037	0.322	0.022
Cu	0.368	0.016	0.371	0.028
Zn	0.677	0.063	0.702	0.067

Validation of CASS-5 coastal seawater reference material. *Original extractions yielded correct value, sample subsequently contaminated

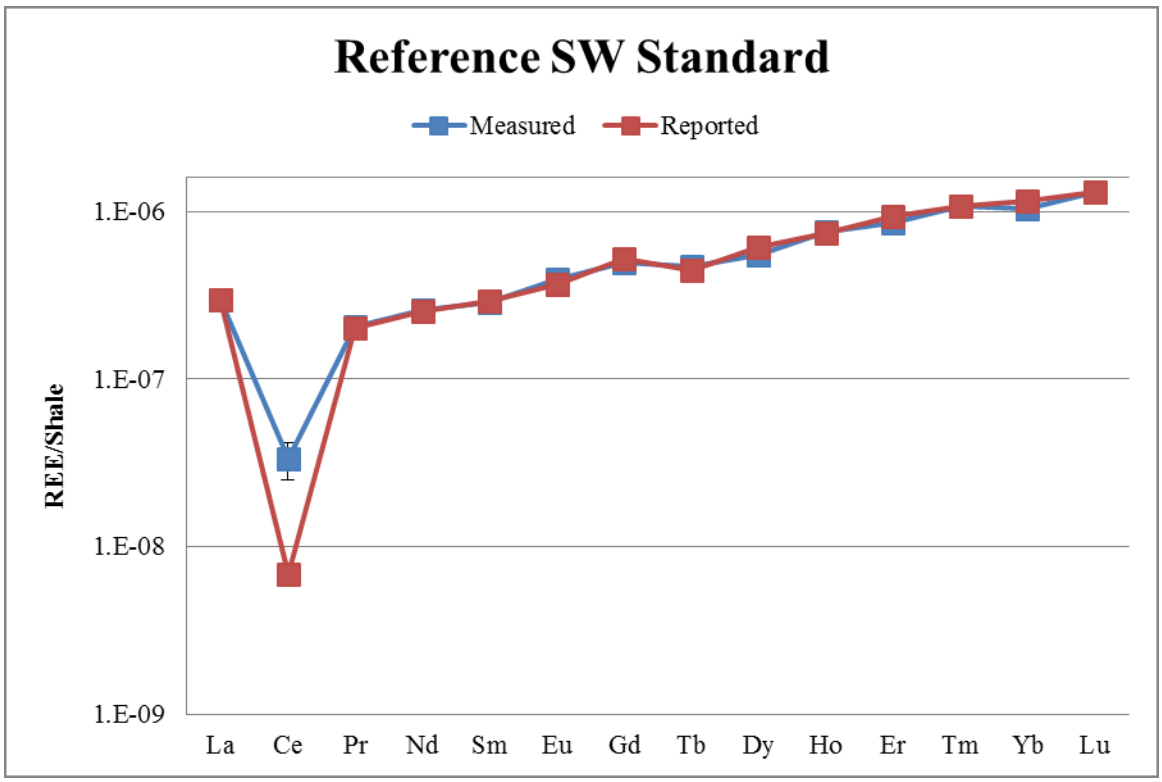

Figure 2.5 Shale normalized REE concentrations of SAFE reference material (KNR195-Nd-8-2158). High cerium was measured repeatedly for sample despite being much high than detection limits. Sample probably contaminated. Reported values based on work by Jeandel lab.

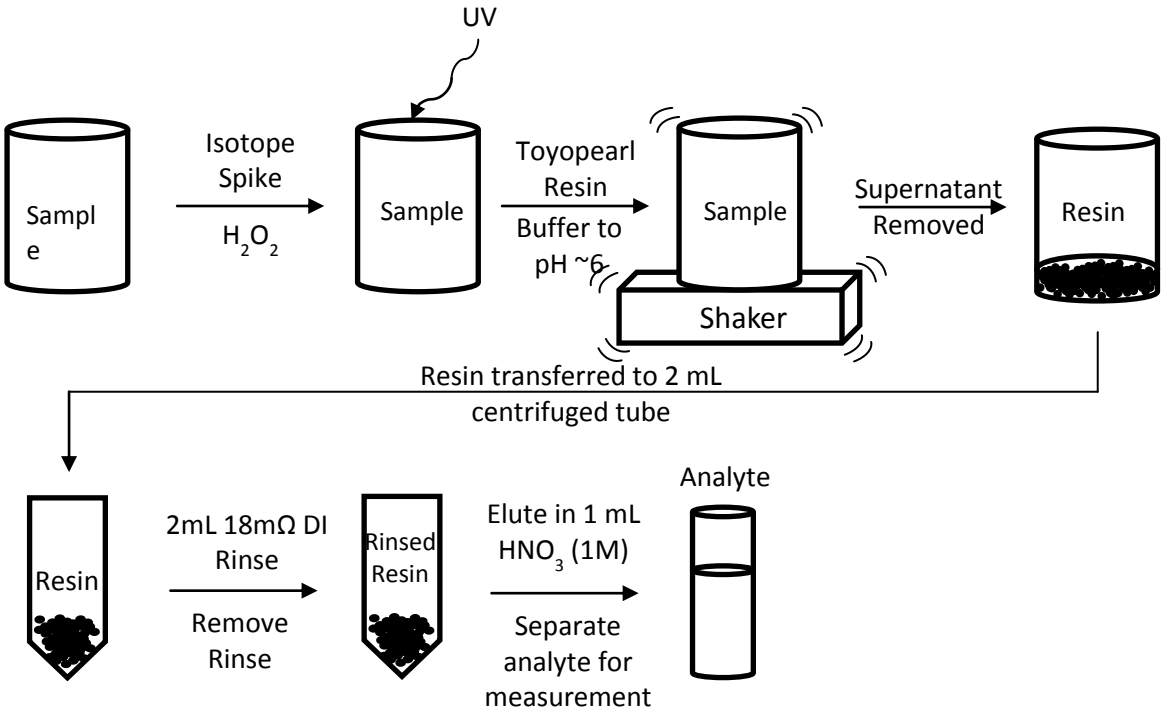

Figure 2.6 Sample processing schematic

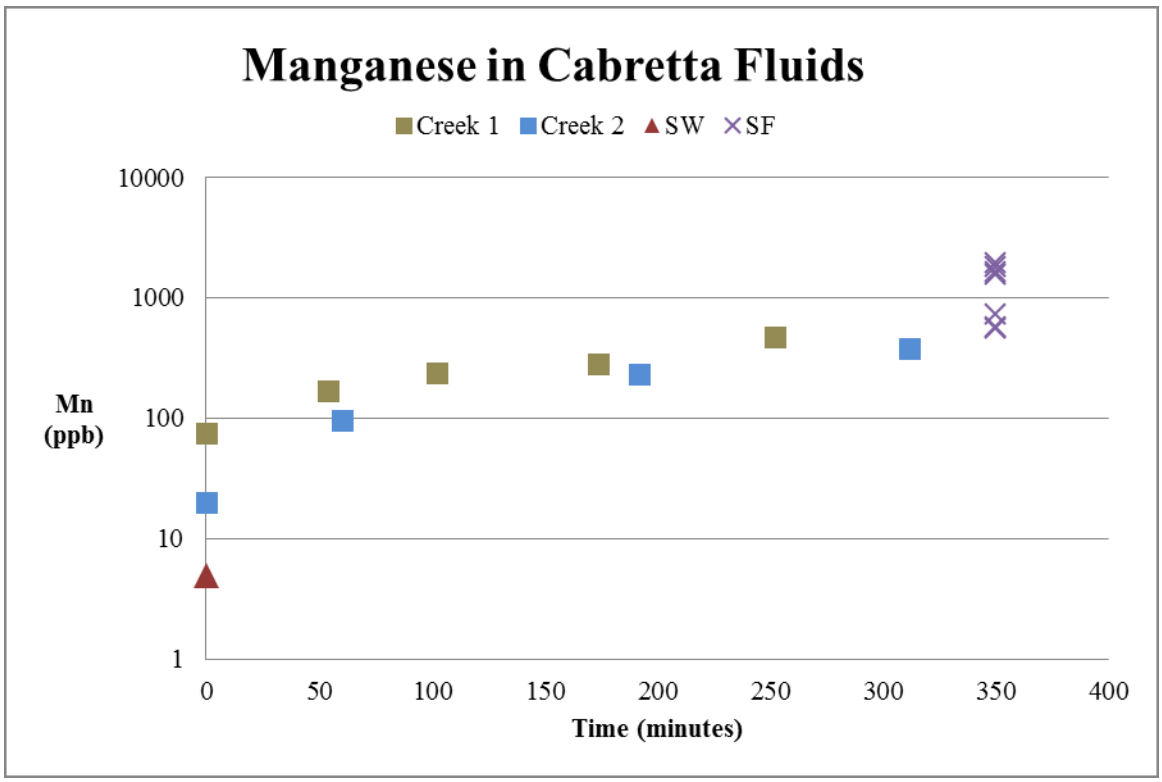

Figure 3.1 Manganese concentrations (ppb) over the ebbing tides in the creek (creek 1 & creek 2), the coastal ocean (SW), and the subterranean fluids (SF).

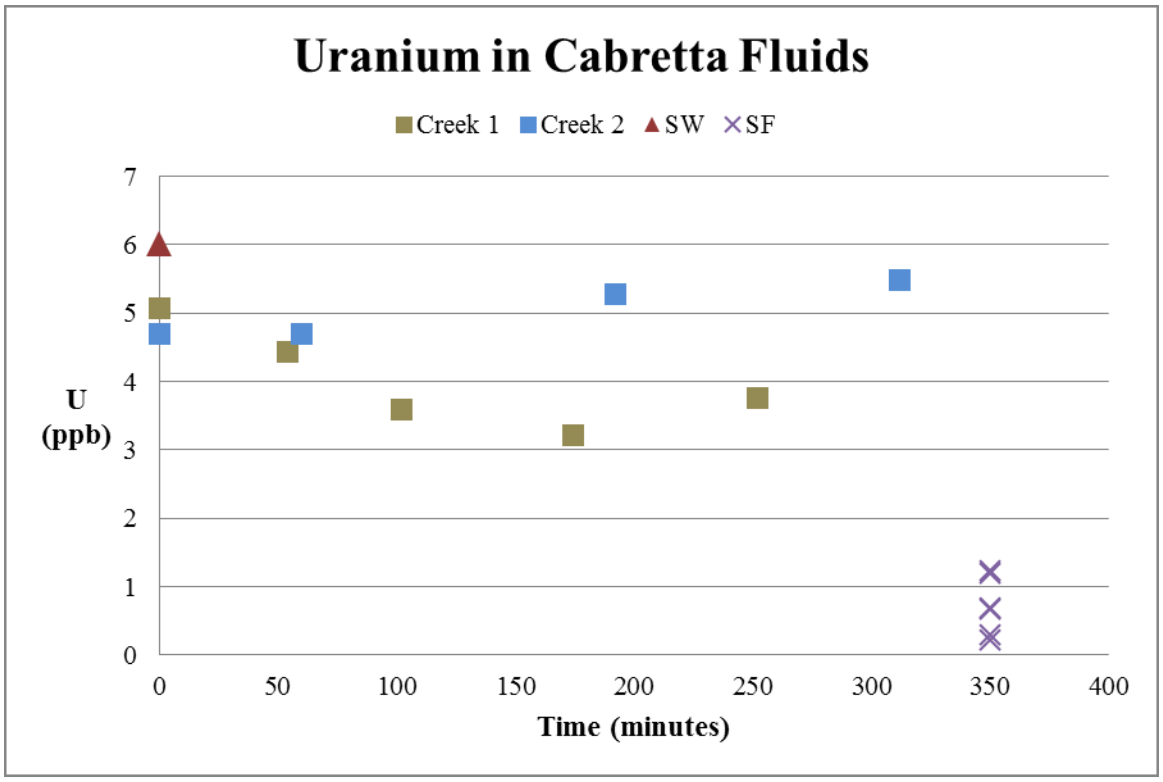

Figure 3.2 Uranium concentrations (ppb) over the ebbing tides in the creek (creek 1 & creek 2), the coastal ocean (SW), and the subterranean fluids (SF).

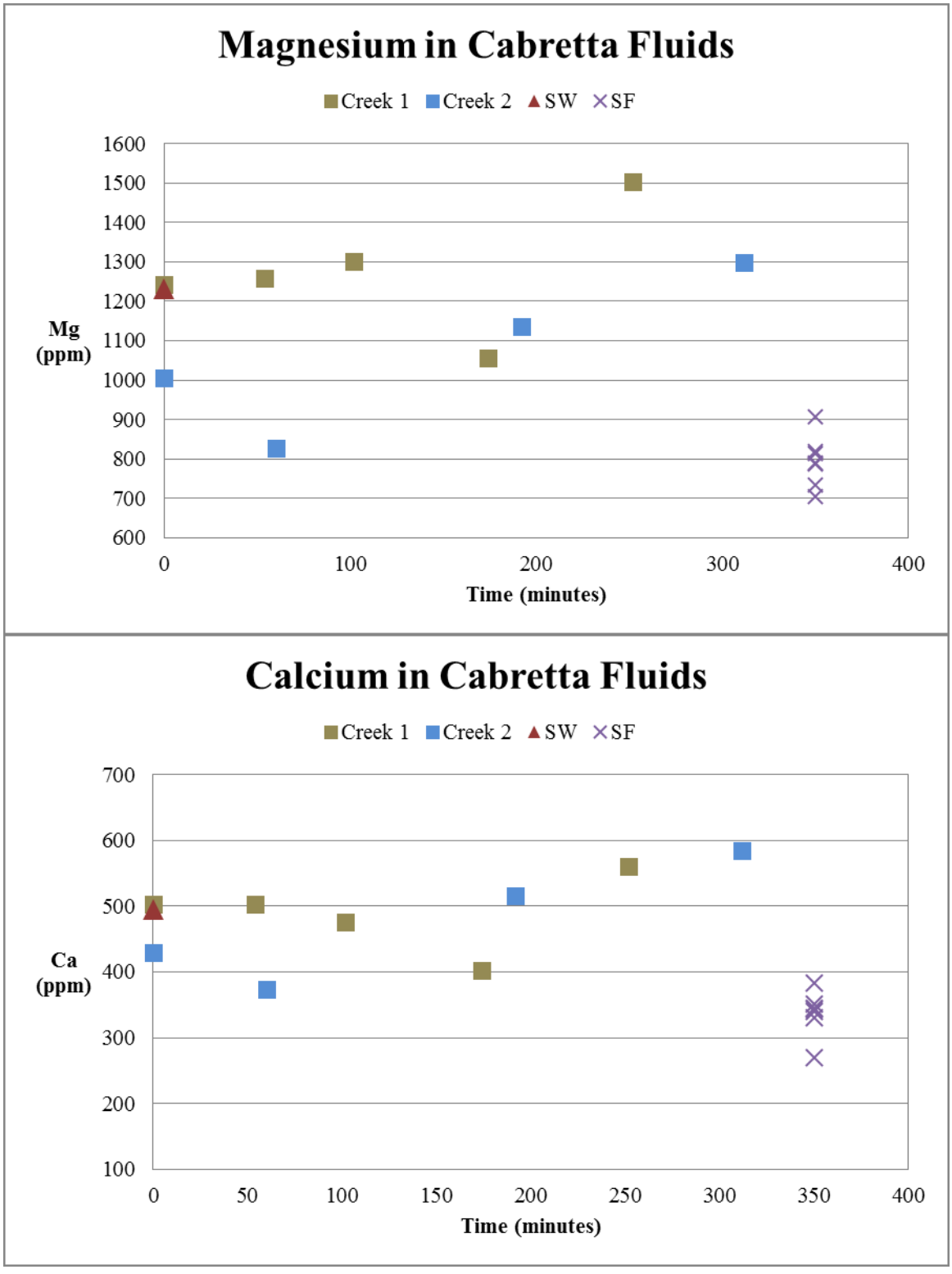

Figure 3.3 Magnesium (top) and calcium (bottom) concentrations (ppb) over the ebbing tides in the creek (creek 1 & creek 2), the coastal ocean (SW), and (SF).

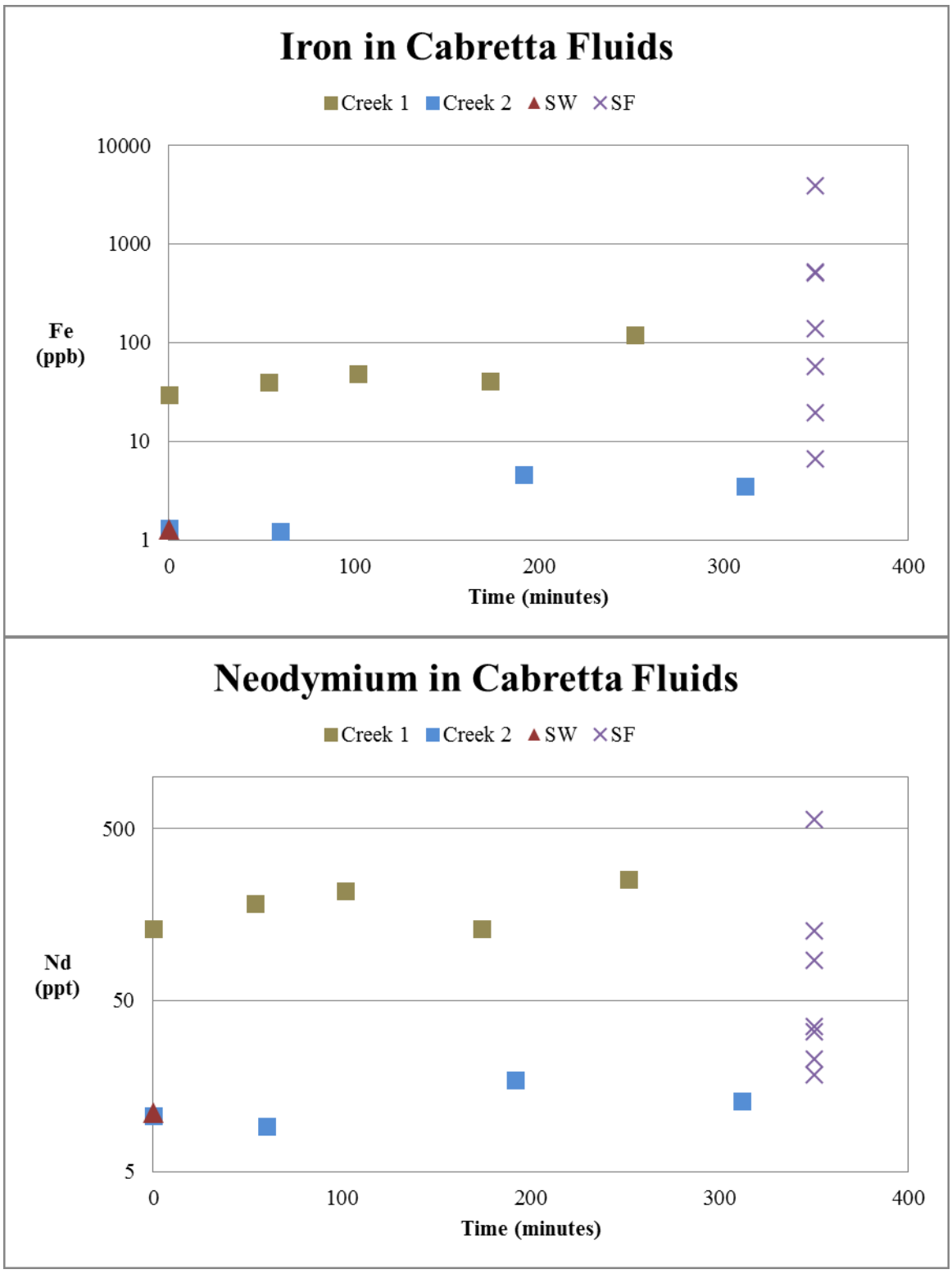

Figure 3.4 Iron (top) and neodymium (REE) (bottom) concentrations (ppb) over the ebbing tides in the creek (creek 1 & creek 2), the coastal ocean (SW), and the subterranean fluids (SF).

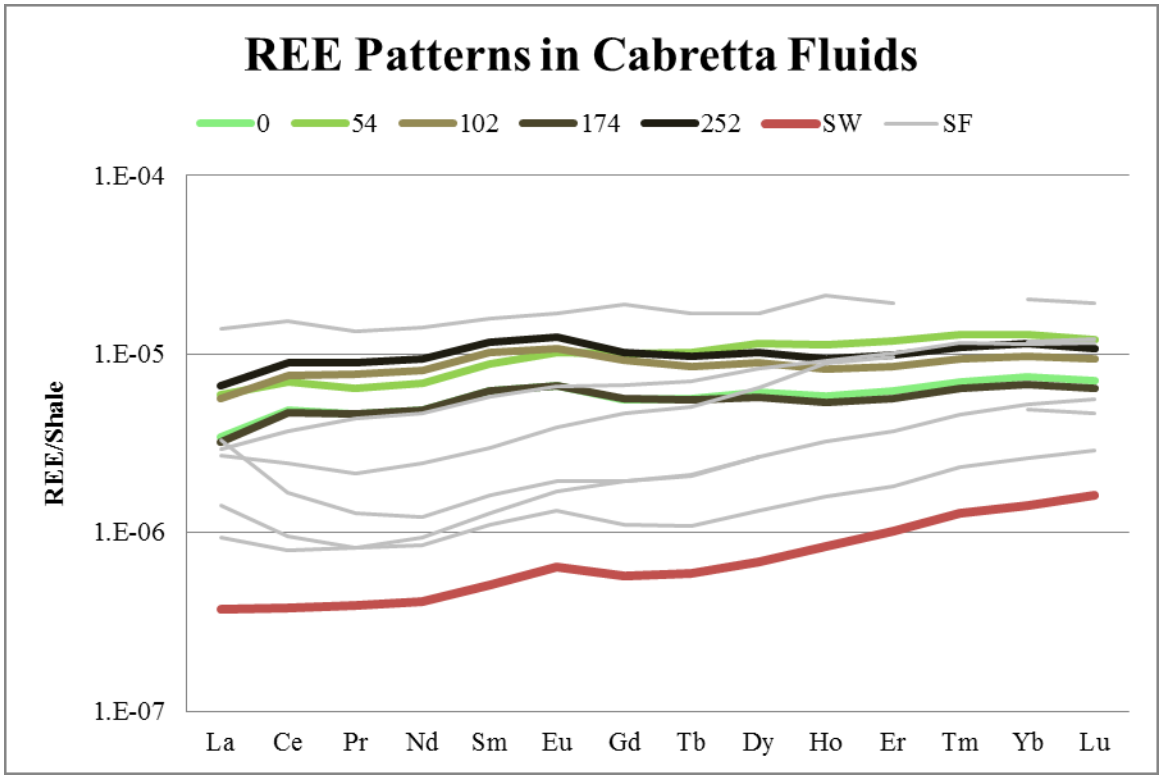

Figure 3.5 REE normalized to shale values over the first ebbing tide, coastal water, and subterranean fluids

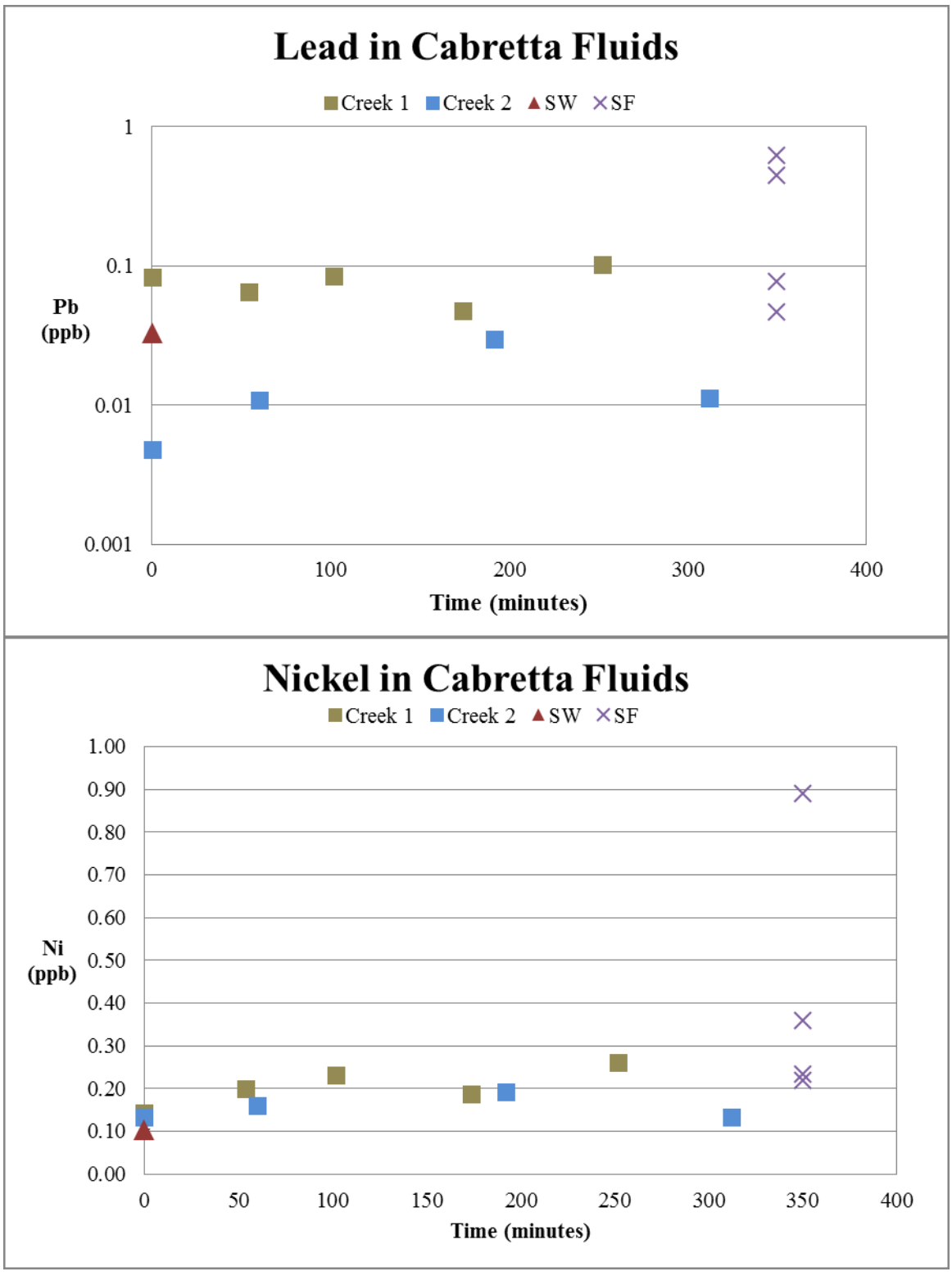

Figure 3.6 Lead (top) and nickel (bottom) concentrations (ppb) over the ebbing tides in the creek (creek 1 & creek 2), the coastal ocean (SW), and the subterranean fluids (SF).

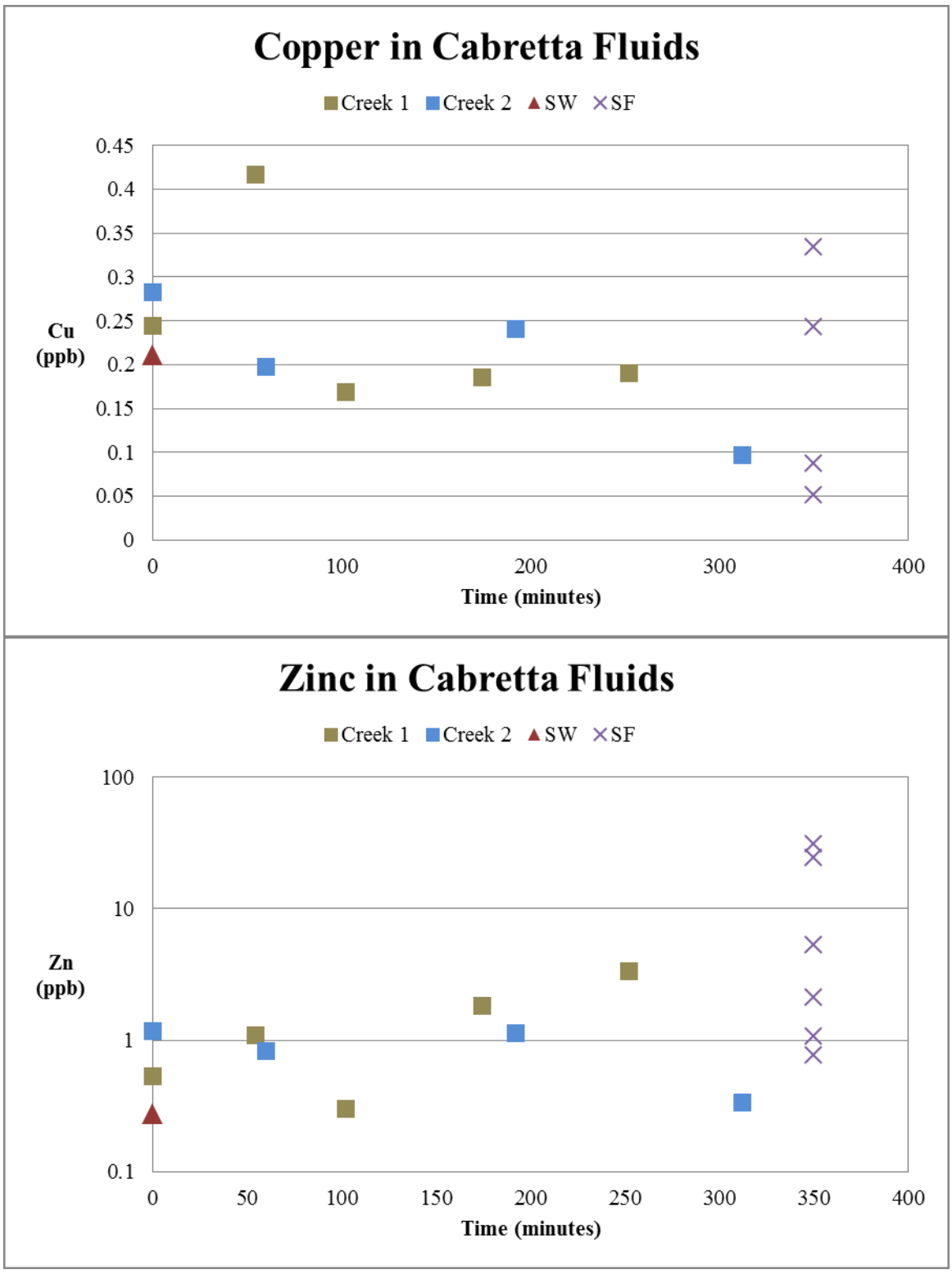

Figure 3.7 Copper (top) and zinc (bottom) concentrations (ppb) over the ebbing tides in the creek (creek 1 & creek 2), the coastal ocean (SW), and the subterranean fluids (SF).

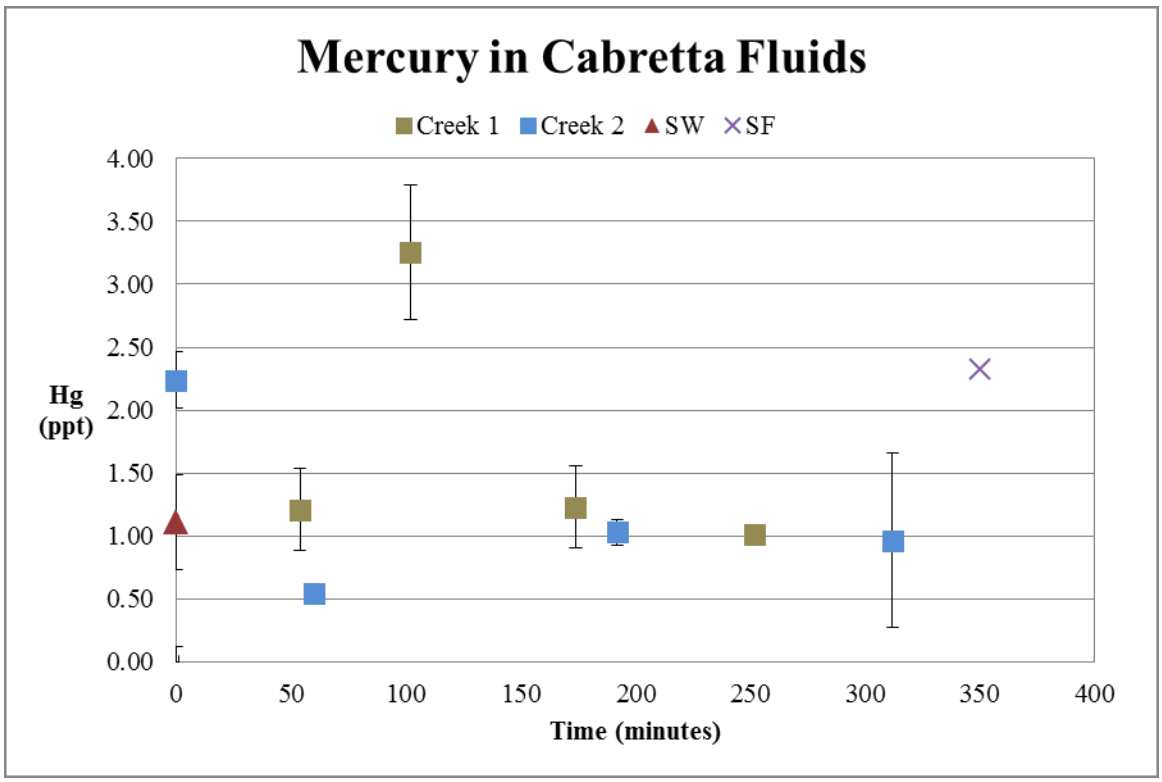

Figure 3.8 Mercury concentrations (ppb) over the ebbing tides in the creek (creek 1 & creek 2), the coastal ocean (SW), and the subterranean fluids (SF). Error bars represent SD for samples with duplicates

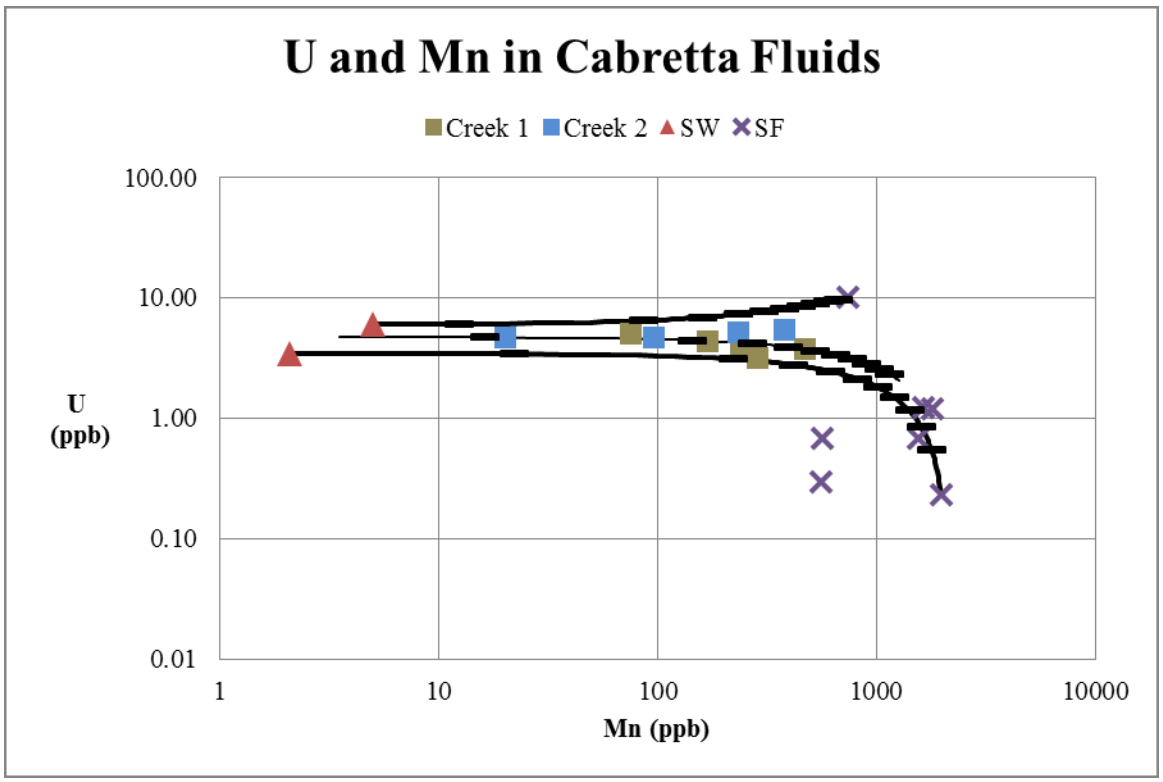

Figure 4.1 Manganese (log scale) and uranium distribution in Cabretta fluids. Black lines represent mixing line between average and outlining end member compositions. Dashes represent 10% intervals of mixing for clarity.

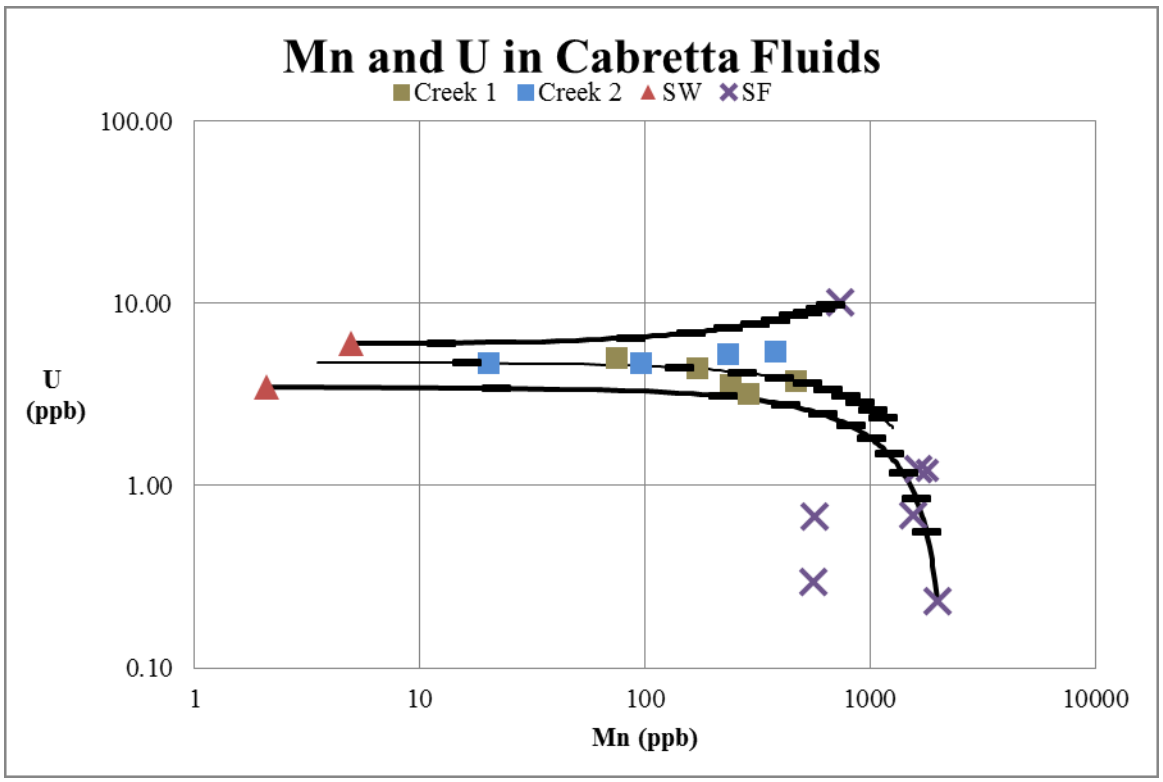

Figure 4.3 Iron and neodymium (log scales) distribution in Cabretta fluids. Black lines represent mixing line between average and outlining end member compositions. Dashes represent 10% intervals of mixing.

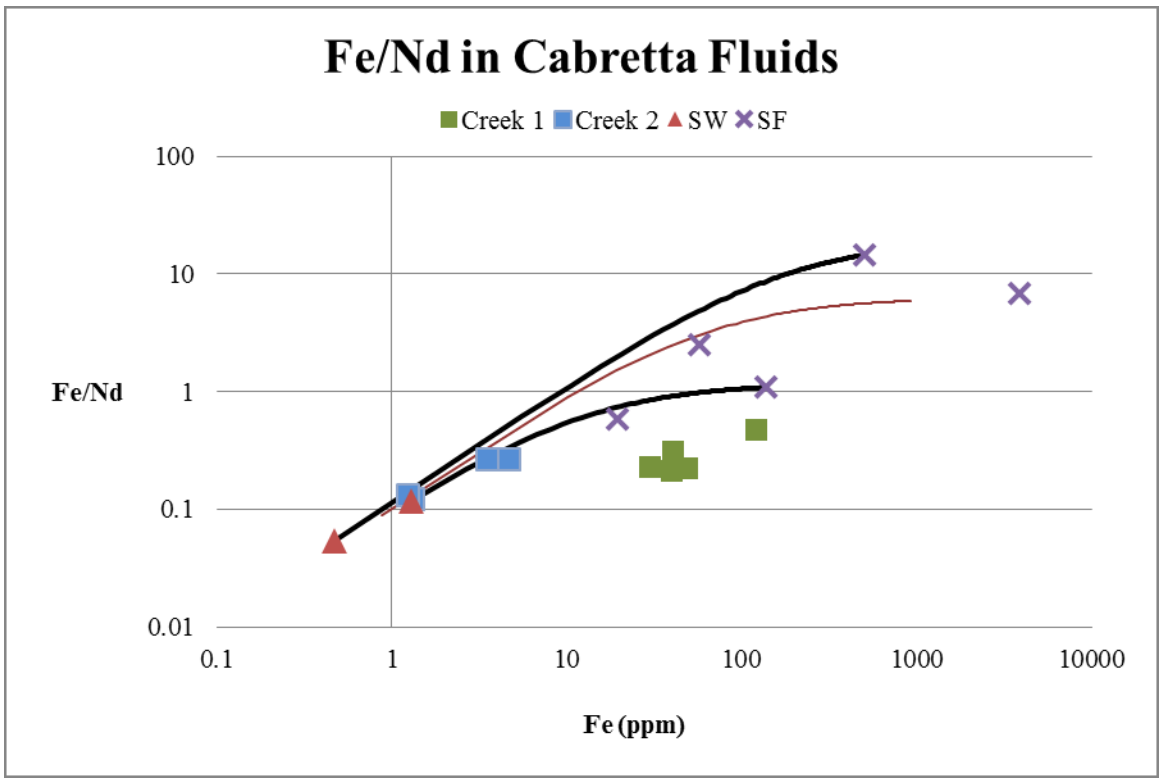

Figure 4.4 Fe/Nd ratios and Fe concentrations (log scales) in the Cabretta fluids. Black lines represent mixing line between average and outlining end member compositions.

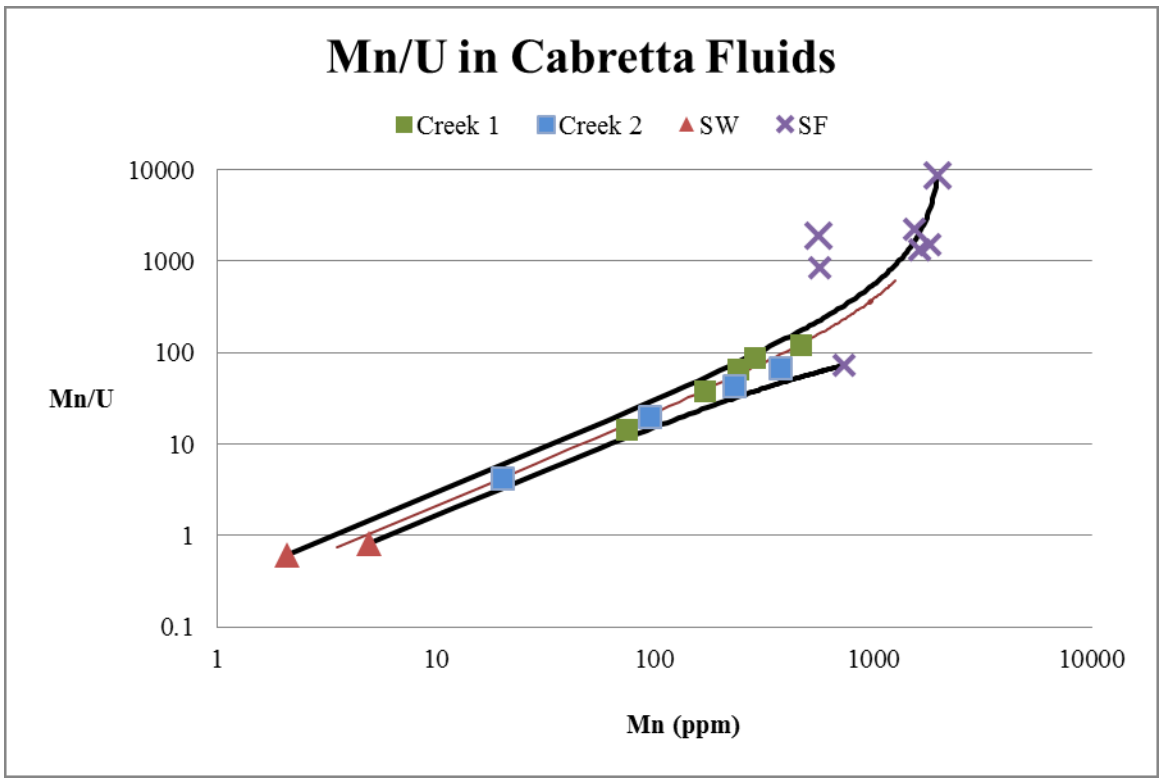

Figure 4.5 Mn/U ratios and manganese concentrations for the Cabretta fluids. Black lines represent average and outlining end-member compositions.

Table 4.1 Tidal Creek Concentrations of Mn in Cabretta End-members (ppb)

Coastal Ocean	Subterranean Fluids
4.98	738.63
2.09	1813.92
	1558.17
	1642.39
	569.87
	561.94
	1983.57

Table 4.2 SF (%) Component in Tidal Creek

	Time (minutes)	SF component in creek	-	+
Creek 1	0	5.74%	1.89%	5.51%
	54	13.20%	4.34%	12.60%
	103	18.80%	6.18%	18.02%
	174	22.44%	7.38%	21.54%
	252	36.94%	12.14%	35.43%
Creek 2	0	1.42%	0.47%	1.37%
	60	7.38%	2.43%	7.09%
	132	18.17%	5.97%	17.43%
	252	29.68%	9.76%	28.47%

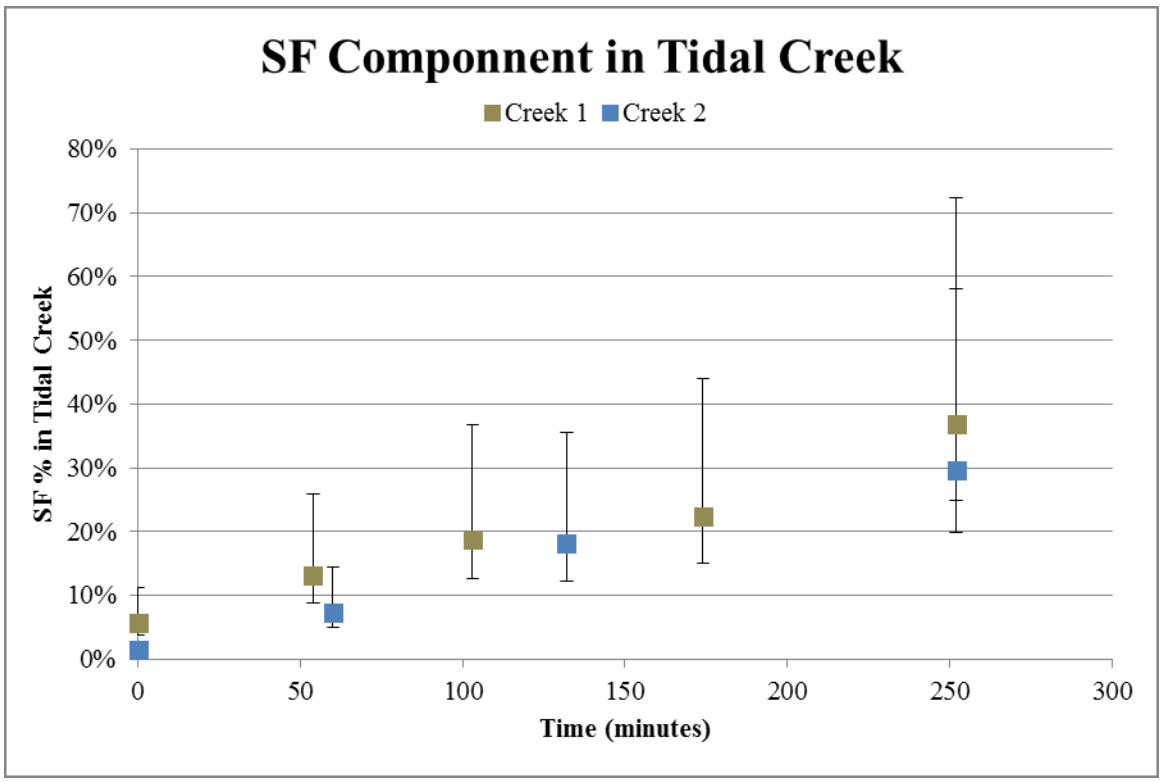

Figure 4.6 Modeled subterranean end member composition (%) based on mixing model of Mn concentrations in Cabretta end members.

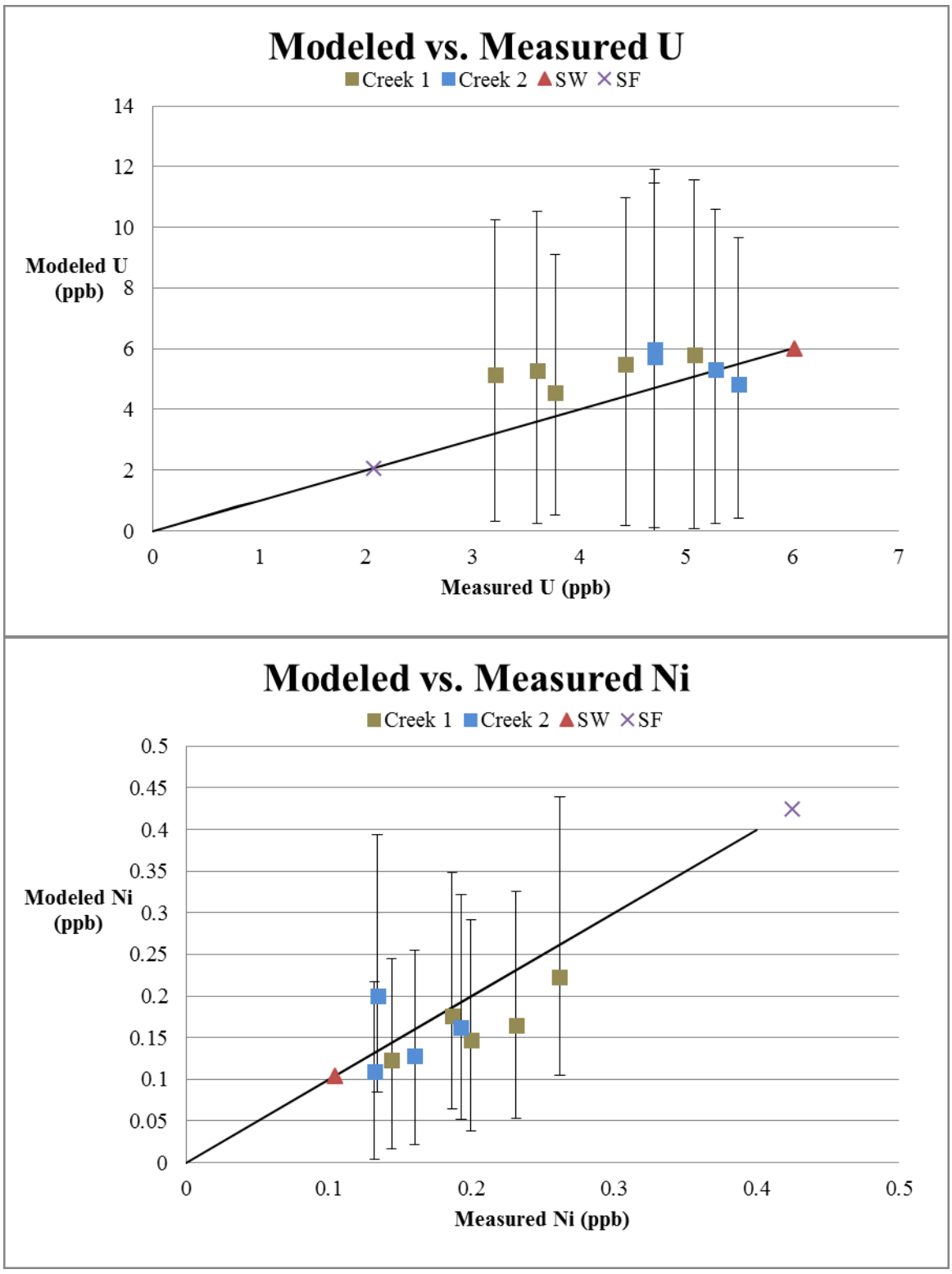

Figure 4.7 Modeled tidal creek concentrations of uranium and nickel. Plotted against measured concentrations. Black line represent 1:1line. 1 standard deviation of SF for modeled concentrations.

Table 4.3 Fluxes* from Cabretta Marsh

	Creek 1	Creek 2	Average Flux	Variability
Mn	427.66	310.50	369.08	22%
U	-3.51	-1.70	-2.61	49.0%
Ni	0.18	0.09	0.13	46.8%
S	-693.96	-125.99	-409.97	98.0%
Fe	95.78	2.43	49.11	134.4%
Mg	68304.20	-292112.41	-111904.11	227.7%
Ca	-9807.23	-32608.23	-21207.73	76.0%
Sr	-482.55	-628.20	-555.37	18.5%
Ba	5828.78	7950.04	6889.41	21.8%
Cd	0.28	0.28	0.28	0.5%

*Fluxes are creek water surface normalized (g/m^2/ebb tide)

Table 4.4 Fluxes* of rare earth elements from Cabretta Marsh

	Creek 1	Creek 2	Average Flux	Variability
La	2.4E-04	1.3E-06	1.2E-04	140%
Ce	6.7E-04	6.9E-07	3.4E-04	141%
Pr	6.7E-07	6.9E-10	3.4E-07	141%
Nd	7.5E-05	2.5E-07	3.8E-05	140%
Sm	6.7E-05	9.9E-07	3.4E-05	137%
Eu	1.5E-05	2.3E-07	7.8E-06	137%
Gd	5.3E-05	1.7E-06	2.7E-05	133%
Tb	9.0E-06	3.4E-07	4.7E-06	131%
Dy	5.4E-05	3.1E-06	2.8E-05	126%
Ho	1.0E-05	8.0E-07	5.6E-06	121%
Er	3.0E-05	3.1E-06	1.7E-05	115%
Tm	4.2E-06	5.1E-07	2.4E-06	111%
Yb	2.9E-05	3.6E-06	1.6E-05	110%
Lu	2.9E-08	3.6E-09	1.6E-08	110%

*Fluxes are creek water surface normalized (g/m^2/ebb tide)

6. References

Adam, P. (1990) Saltmarsh Ecology, Cambridge University Press

Beck, A.J., Tsukamoto, Y., Tocar-Shanchez, A., Huerta-Diaz, M., Bokuniewicz, H.J., & Sañudo-Wilhelmy, S.A., (2006) Important of geochemical transformations in determining submarine groundwater discharge-derived trace metal and nutrient fluxes, Applied Chemistry **22**, 477-490.

Das, R., Bizimis, M., and Wilson, A.M., (2012) Tracing mercury seawater vs. atmospheric inputs in a pristine SE USA salt marsh system: Mercury isotope evidence, Chemical Geology **336**, 50-61.

Charette, M.A. and Sholkovitz, E.R., (2006) Trace element cycling in a subterranean estuary: Part 2. Geochemistry of the pore water, Geochimica et Cosmochimica **70**, 811-826.

Church, T.M., Sarin, M.M., Fleisher, M.Q., and Ferdelman, T.G. (1996) Salt Marshes: An important coastal sink for dissolved uranium, Geochimica et Cosmochimica **60**, 3879-3887.

Duncan, T. and Shaw, T.J. (2004) The mobility of rare earth elements and redox sensitive elements in the groundwater/seawater mixing zone of a shallow coastal aquifer, Aquatic Chemistry **9**, 233-255.

Elderfield, H. and Greaves, M.J., (1982) The rare earth elements in sea water, Nature **296**, 214-219.

Elderfield, H. and Sholkovitz, E.R., (1987) Rare earth elements in the pore waters of reducing nearshore sediments, Earth and Planetary Science Letters **82**, 280-288.

Freslon, N., Bayon, G., Birot, D., Bolinger, C., Barrat, J. A., (2011) Determination of rare earth elements and other trace elements (Y, Mn, Co, Cr) in seawater using Tm addition and $Mg(OH)_2$ co-precipitation, Talanta **85**, 582-587.

Giblin, A.E., (1984) Porewater evidence for a dynamic sedimentary iron cycle in salt marshes, Limnology and Oceanography **29**, 27-63.

Gillham, M.E., (1957) Vegetation of the exe estuary in relation to water salinity, Journal of Ecology **45**, 735-756.

Haines, E.B., (1979) Food sources of estuarine invertebrates analyzed using C^{13}/C^{12} ratios, Journal of Ecology **60**, 58-56.

Johannesson, K.H., Chevis, D.A., Burdige, D.J., Cable, J.E., Martin, J.B., Roy, M.,(2011) Submarine groundwater discharge is an important net source of light and middle REEs to coastal waters of the Indian River Lagoon, Florida, USA, Geochimica et Cosmochimica **75**, 825-843.

Koretsky, C.M., Cuellar, A., Haveman, M., Beuving, L., Shattuck, T., & Wagner, M., (2008) Influence of Spartina and Juncus on saltmarsh sediments. I. Pore water geochemistry, Chemical Geology **255**, 87-99.

Koretsky, C.M., Cuellar, A., Haveman, M., Beuving, L., Shattuck, T., & Wagner, M., (2008) Influence of Spartina and Juncus on saltmarsh sediments. II. Trace element geochemistry, Chemical Geology **255**, 100-113.

Lee, G., Bigham, J.M., and Faure, G., (2001) Removal of trace metals by coprecipitation with Fe, Al, and Mn, from natural waters contamined with acid mine drainage in the Ducktown Mining District, Tennesee, Applied Geochemistry **17**, 569-581.

Milne, A., Landing, W., Bizimis, M., and Morton, P., Determination of Mn, Fe, Co, Ni, Cu, Zn, and Pb, in seawater using high resolution magnetic selector inductively coupled mass spectrometry (HR-ICP-MS), Geochimica et Cosmochimica **665**, 200-207.

Moore, W.S., (1999) The subterranean estuary: a reaction zone of ground water and sea water, Marine Chemistry **65**, 111-125.

Pahnke, K., Van de Flierdt, T., Jones, K. M., Lambelet, M., Hemming, S.R., (2012) GEOTRACES intercalibration of neodymium isotopes and rare earth element concentrations in seawater and suspended particles. Part 2: Systematic tests and baseline profiles, Limnology and Oceanography: Methods **10**, 252-260.

Runick, R.L. and Goa, S., (2003) Composition of the continental crust, Treatise of Geochemistry **3**, 1-64.

Santos-Echeandía, J., Vale, C., Caetano, M., Pereira, P., & Prego, R., (2010) Effect of tidal flooding on the metal distribution of pore waters of marsh sediments and its transport to the water column (Tagus estuary, Portugal), Marine Environment Research **70**, 358-367.

Seeberg-Elverfeldt, J., Schulter, M., Feseker, T., & Kolling, M., (2005) Rhizon sampling of porewaters near the sediment-water interface of aquatic systems, Limnology and Oceanography: Methods **3**, 361-371

Stumpf, R.P., (1983) The process of sedimentation on the surface of a salt marsh, Estuarine, Coastal, and Shelf Science **17**, 495-508.

Taillefert, M., Neuhuber, S., & Bristow, G., (2007) The effect of tidal forcing on biogeochemical processes in intertidal salt marsh sediments, Geochemical Transactions **8:6**

Valiela, I., (1978) Nutrient and particulate fluxes in a salt marsh ecosystem: Tidal exchanges and inputs by precipitation and groundwater, Limnology and Oceanography **23**, 798-812.

Wilson, A.M., and Moore, W.S., Joye, S.B., Anderson, J.L., & Schutte, C.A., (2011) Storm-driven groundwater flow in a salt marsh, Water Resources Research **47**, 1-118.